



Available online at www.sciencedirect.com

ScienceDirect

Comput. Methods Appl. Mech. Engrg. 334 (2018) 483–506

**Computer methods
in applied
mechanics and
engineering**

www.elsevier.com/locate/cma

The effect of prior probabilities on quantification and propagation of imprecise probabilities resulting from small datasets

Jixin Zhang, Michael D. Shields*

Department of Civil Engineering, Johns Hopkins University, Baltimore, MD 21218, USA

Received 8 September 2017; received in revised form 3 January 2018; accepted 24 January 2018

Available online 10 February 2018

Abstract

This paper outlines a methodology for Bayesian multimodel uncertainty quantification (UQ) and propagation and presents an investigation into the effect of prior probabilities on the resulting uncertainties. The UQ methodology is adapted from the information-theoretic method previously presented by the authors (Zhang and Shields, 2018) to a fully Bayesian construction that enables greater flexibility in quantifying uncertainty in probability model form. Being Bayesian in nature and rooted in UQ from small datasets, prior probabilities in both probability model form and model parameters are shown to have a significant impact on quantified uncertainties and, consequently, on the uncertainties propagated through a physics-based model. These effects are specifically investigated for a simplified plate buckling problem with uncertainties in material properties derived from a small number of experiments using noninformative priors and priors derived from past studies of varying appropriateness. It is illustrated that prior probabilities can have a significant impact on multimodel UQ for small datasets and inappropriate (but seemingly reasonable) priors may even have lingering effects that bias probabilities even for large datasets. When applied to uncertainty propagation, this may result in probability bounds on response quantities that do not include the true probabilities.

© 2018 Elsevier B.V. All rights reserved.

Keywords: Uncertainty quantification; Data-driven; Imprecise probability; Prior probabilities; Multimodel inference; Bayesian inference

1. Introduction

Uncertainty quantification (UQ) is the science of quantitatively characterizing and, if possible, reducing uncertainties in the computational evaluation of engineering/mathematical systems. It is used to determine how likely certain outcomes are if some parts of the system are not exactly known. Practically speaking, UQ is playing an increasingly important role in performance prediction, reliability analysis, risk evaluation and decision making. Uncertainty can be broadly classified into two categories [1]: *epistemic*, resulting from a lack of complete knowledge and modeling approximations, and *aleatory*, resulting from inherent randomness. It is widely accepted that probability theory

* Corresponding author.

E-mail addresses: jixin.zhang@jhu.edu (J. Zhang), michael.shields@jhu.edu (M.D. Shields).

provides an appropriate framework for the treatment of aleatory uncertainty although it is open to debate as to what mathematical treatment is most appropriate for epistemic uncertainty.

It is often considered preferable to view all uncertainty probabilistically — given the well-understood and intuitive nature of probability theory. This desire has given rise to the field of so-called imprecise probabilities wherein aleatory uncertainties are modeled using standard probability theory and epistemic uncertainties provide a level of “imprecision”. Despite efforts to develop a unified theory of imprecise probability [2,3], there remain numerous approaches to model this imprecision that include the use of random sets [4–6], intervals and probability boxes [7–11], Bayesian [12,13] and frequentist [14,15] methods, and combinations of these theories [16,17] among many others (e.g. [18]). Additionally, Dempster–Shafer theory [19,20] and fuzzy set theory [21] aim to relax the constraints on probability measures to account for this imprecision. For the interested reader, an extensive review of many of these approaches for engineering applications can be found in [22].

In this work, we apply a multimodel Bayesian probabilistic approach, extended from [23], to quantify and propagate combined aleatory and epistemic uncertainty. Specifically, epistemic uncertainties manifest as uncertainties in the form of probability models characterizing a dataset (referred to as *model-form uncertainties* or *structural uncertainties* [24]) and uncertainties in the parameters of the probability models (referred to as *parameter uncertainties*). Both model-form and parameter uncertainties are quantified from the given data using Bayesian inference. The result of this multimodel approach is a set of candidate probability models (each having associated probability) and the joint parameter probability densities for each model that provides a near comprehensive description of the uncertainties in the system rooted in probabilities (or more precisely probabilities of probabilities).

The imprecise probabilities quantified using the proposed approach are propagated through a model of a physical system using a Monte Carlo approach with importance sampling reweighting for simultaneous propagation of the full set of probability models [23]. The procedure is critical in reducing the computational expense of Monte Carlo-based imprecise probability propagation by reducing a multi-loop Monte Carlo to a single-loop Monte Carlo.

Given that the approach employed herein is fully Bayesian in its construction and the datasets used for inference are necessarily small, prior probabilities are likely to influence the quantified uncertainties in important ways. The primary objective of this work is to improve our understanding of the influence of prior probabilities in both model-form and parameter uncertainties on the quantified uncertainties and, ultimately, on propagated uncertainties. We employ informative and noninformative priors for both model-form and parameter uncertainties under realistic data availability constraints. More specifically, priors are formulated based on either assumed ignorance (noninformative) or using historical data available from literature (informative) that may or may not be entirely appropriate for the present analysis. In other words, the informative prior may be incorrect in seemingly subtle ways. This is combined with the reality of small datasets for Bayesian inference used for quantifying imprecise probabilities and, an example of a simple plate buckling problem with uncertainty in material properties is used to illustrate how prior probabilities come to have a strong influence (good or bad) on multimodel uncertainty quantification and propagation from small datasets. Moreover, the effect of the prior is studied to observe, for this application, the rate of convergence of imprecise probabilities to the “true” probabilities for increasing dataset size. Even in these large data case, it is shown that seemingly rational (but ultimately incorrect) priors can create biases that preclude convergence to the true probabilities.

The paper is structured as follows. Sections 2 and 3 provide the basic theory for multimodel Bayesian uncertainty quantification for model-form (Section 2) and parameter uncertainties (Section 3). Section 4 reviews a new Monte Carlo-based method for multimodel uncertainty propagation proposed in a recent work by the authors [23]. Some minor modifications are included. Section 5 discusses the formulation of model and parameter prior probabilities. The influence of these prior probabilities on multimodel uncertainty quantification and propagation is then studied in the context of a simplified plate buckling problem in Section 6 where priors are considered to be either noninformative or rooted in historical data from literature. Several such priors are considered for both model-form and parameter uncertainties and their influence studied systematically. Finally, some concluding remarks are provided in Section 7.

2. Bayesian multimodel inference and model-form uncertainty

Among the most important problems in computational science and engineering are the quantification of model-form uncertainty and its use for model selection, with widespread recognition of these challenges dating back for more than 30 years [25,26]. Probabilistic model selection has taken considerable strides forward with the development of approaches based on Bayes’ theory and information theory. Bayesian approaches involving the notion of posterior

model probabilities follow the work of Raftery [12] and have been revived in the more recent work of Beck [27–29] and Oden [30–32]. Meanwhile the information-theoretic approach is derived from the work of Akaike [33,34] and its further generalizations [35–37].

The issue of model selection is fundamental to the quantification of input uncertainties for physics-based calculations given limited data. In such cases, multiple probability models may reasonably fit the data. Generally, either the Bayesian and information-theoretic model selection methods are employed to select a single “best” model based on the given data and a set of candidate models. That model is then the sole model used for uncertainty propagation without any further consideration for the assessment and propagation of model-form uncertainty [25,24]. This approach is known to potentially misrepresent the true uncertainties in statistical quantities of interest (typically underestimating them) [24], while also implicitly asserting that a “true” model exists, which is counter to the definition of a model [38]. In certain cases, model averaging is performed (see [39] and the associated commentary) and, while this may be preferable, it still ignores much of the true model-form uncertainty by propagating only averaged quantities rather than their full probability structure. Moreover, such selection needs very large datasets. Given scarcity of data, it is often impossible to identify a unique best model so that we need to quantify model-form uncertainty and retain multiple candidate models and their associated probabilities — a method referred to as multimodel inference [40]. The previous work of the authors [23] presented an information-theoretic approach for multimodel inference to quantify and propagate these model-form uncertainties. This work seeks to generalize this in a fully Bayesian framework.

2.1. Bayesian multimodel inference

In this work, we consider the specific case of probability model selection from sparse data. In all subsequent discussion, a model M_i refers to a parametric probability model for a random variable X (typically expressed in the form of a probability density function, $p(x)$) having parameters θ_i . Given a collection of m candidate models $\mathcal{M} = \{M_j\}$ with model parameters θ_j , $j = 1, \dots, m$, our objective in this section is to assess the “goodness-of-fit” of each model given a dataset \mathbf{d} of independent observations of X and ultimately infer probabilities that each model is the “best” model for the data.

In the Bayesian setting, selection between two models M_i and M_j given data \mathbf{d} is often performed by estimating the ratio of posterior odds as

$$\underbrace{\frac{p(M_i|\mathbf{d})}{p(M_j|\mathbf{d})}}_{\text{Posterior odds}} = \underbrace{\frac{p(M_i)}{p(M_j)}}_{\text{Prior odds}} \times \underbrace{\frac{p(\mathbf{d}|M_i)}{p(\mathbf{d}|M_j)}}_{\text{Bayes' factor}} \quad (1)$$

where Bayes’ factor is defined as the ratio of the evidence of M_i and M_j , and the prior odds is the ratio of model prior of M_i and M_j . If the posterior odds are greater than one, then model M_i is selected while if the posterior odds are less than one, model M_j is selected.

Intuitively, Bayes’ factor can be easily generalized for comparison of multiple candidate models. Consider the aforementioned collection of m parametric models \mathcal{M} , with each model M_j having an associated prior probability $\pi_j = p(M_j)$ with $\sum_{j=1}^m \pi_j = 1$. Bayes’ rule relates posterior model probabilities $\hat{\pi}_j$ to prior model probabilities π_j via the formula

$$\hat{\pi}_j = p(M_j|\mathbf{d}) = \frac{p(\mathbf{d}|M_j)p(M_j)}{\sum_{k=1}^m p(\mathbf{d}|M_k)p(M_k)}, \quad j = 1, \dots, m \quad (2)$$

having $\sum_{j=1}^m \hat{\pi}_j = 1$ and where

$$p(\mathbf{d}|M_j) = \int_{\Theta_j} p(\mathbf{d}|\theta_j, M_j)p(\theta_j|M_j)d\theta_j, \quad j = 1, \dots, m \quad (3)$$

is the marginal likelihood or evidence of model M_j . Typically, the model $M_k \in \mathcal{M}$ with highest probability $p(M_k|\mathbf{d})$ is deemed the most plausible in the set \mathcal{M} for the given data \mathbf{d} . In the multimodel inference context, rather than selecting the model with the highest probability, the models are ranked according to their probabilities given by Eq. (2) and all models with non-negligible probability are retained.

In Bayesian parameter estimation the evidence $p(\mathbf{d}|M_j)$ is just a normalization factor that does not need to be evaluated explicitly using Markov Chain Monte Carlo (MCMC). However, as evident from Eq. (2), the evidence $p(\mathbf{d}|M_j)$ is critical in Bayesian multimodel inference and consequently needs to be calculated with caution. The following section discusses evidence calculation.

2.2. Bayesian evidence calculation

The evidence in Eq. (3) can be computed in a number of different ways. In rare cases, the integral can be evaluated analytically. Usually, approximate or statistically exact (i.e. Monte Carlo) methods are necessary.

One efficient approximation uses Laplace's approach [37] to approximate the evidence $p(\mathbf{d}|M_j)$ as

$$p(\mathbf{d}|M_j) \approx \exp\{\log(p(\mathbf{d}|\boldsymbol{\theta}_j^*, M_j))\} p(\boldsymbol{\theta}_j^*|M_j) (2\pi)^{K_j/2} n^{-K_j/2} |H^*(\boldsymbol{\theta}_j^*)|^{-1/2}. \quad (4)$$

Taking the logarithm of this expression and multiplying it by -2 , we obtain

$$-2 \log(p(\mathbf{d}|M_j)) \approx -2 \log(p(\mathbf{d}|\boldsymbol{\theta}_j^*, M_j)) + K_j \log(n) + \log|H^*(\boldsymbol{\theta}_j^*)| - K_j \log(2\pi) - 2 \log(p(\boldsymbol{\theta}_j^*|M_j)) \quad (5)$$

where K_j is the dimension of the parameter vector $\boldsymbol{\theta}$, $\boldsymbol{\theta}_j^*$ is the maximum likelihood estimate and H^* is the inverse Hessian of the negative log likelihood (Fisher information matrix). Ignoring the terms in Eq. (5) with order less than $O(1)$ with respect to the large sample size n yields the Bayesian Information Criteria (BIC) [35]

$$\text{BIC}_j = \text{BIC}(M_j) = -2 \log(p(\mathbf{d}|\boldsymbol{\theta}_j^*, M_j)) + K_j \log(n) \quad (6)$$

where n is the dataset size. This quantity can be used to construct an asymptotic approximation to Bayes' factor, namely $\text{BF}_{i,j} \approx \exp(-(\text{BIC}_i - \text{BIC}_j))/2$ [12]. Combined with the model prior $\pi_j = p(M_j)$, posterior model probabilities from Eq. (2) can be expressed as

$$\hat{\pi}_j^{\text{BIC}} \approx \frac{\exp(-\frac{1}{2}(\text{BIC}_j - \text{BIC}_{\min}))\pi_j}{\sum_{k=1}^m \exp(-\frac{1}{2}(\text{BIC}_k - \text{BIC}_{\min}))\pi_k} \quad (7)$$

where $\text{BIC}_{\min} = \min_j(\text{BIC}_j)$. Assigning uniform prior model probabilities to the set \mathcal{M} , $\pi_j \equiv 1/m$, yields what are referred to as BIC model weights. In fact, Eq. (7) can be considered generalized BIC model weights for arbitrary prior model probabilities. Notice also that Eq. (6) may be thought of as an implicit approximation of evidence $p(\mathbf{d}|M_j)$ under a *noninformative parameter prior* (or *Jeffreys parameter prior*) even though it does not explicitly depend on a parameter prior.

The information-theoretic multimodel selection (introduced in [40] and employed in the authors' previous work [23]) can be shown as a special case of the Bayesian evidence-based multimodel selection used herein. Akaike [33] showed that the maximized log-likelihood is a biased estimator of the K-L information and that the bias is approximately equal to K_j . Hence, the Akaike Information Criterion (AIC) is defined

$$\text{AIC}_j = \text{AIC}(M_j) = -2 \log(p(\mathbf{d}|\boldsymbol{\theta}_j^*, M_j)) + 2K_j \quad (8)$$

as an approximation of the K-L information. By rescaling the AIC as

$$\Delta_j = \text{AIC}_j - \text{AIC}_{\min} \quad (9)$$

the marginal likelihood of the model M_j given the data can be expressed as $\exp(-\frac{\Delta_j}{2})$, $j = 1, \dots, m$ [41]. By normalizing these likelihoods to sum to 1, they are treated as model probabilities (as in Eq. (7)) with

$$\hat{\pi}_j^{\text{AIC}} = \frac{\exp(-\frac{\Delta_j}{2})}{\sum_{k=1}^m \exp(-\frac{\Delta_k}{2})}. \quad (10)$$

As shown by [40], Eq. (10) is in fact a special case of Eq. (7) in which the prior model probabilities π_j take the form

$$\pi_j = \frac{\exp(\frac{1}{2}K_j \log(n) - K_j)}{\sum_{k=1}^m \exp(\frac{1}{2}K_k \log(n) - K_k)}. \quad (11)$$

These forms of priors are referred to as *savvy* (shrewdly informed) priors because they depend on n and K_k .

The BIC and AIC based results are important because they illustrate directly the influence of priors in the asymptotic case. While the model probabilities in Eq. (2) are general, they can be approximated (in large data cases) by Eq. (7) and the AIC derived model probabilities are an instance of this approximation under certain prior information.

Because both the BIC and AIC are asymptotic quantities that require large dataset size, they are of limited practical use here. Although a small data correction of the AIC, denoted AICc, has been derived [36,42] and used in our

previous work [23], this again implies a certain prior form and our objective here is to investigate the effect of the prior. Consequently, we must rely on other estimators for Eq. (3) that do not have asymptotic conditions or assume a prior form. We favor a Monte Carlo-based statistical estimator given by

$$\hat{p}(\mathbf{d}|M_j) = \frac{1}{N_k} \sum_{k=1}^{N_k} p(\mathbf{d}|\boldsymbol{\theta}_j^k, M_j), \quad \boldsymbol{\theta}_j^k \sim p(\boldsymbol{\theta}_j|M_j), \quad j = 1, \dots, m \quad (12)$$

in which samples $\boldsymbol{\theta}_j^k$ are drawn from the parameter prior distribution and N_k is the number of samples. The computational cost of the Monte Carlo-based algorithm for probability models used in this paper is moderate, and its efficiency can be improved with parallel computing. For complex or high dimensional model evidence calculation, MCMC-based algorithms, including Chib and Jeliazkov [43] and nested sampling [44] may be preferable as discussed in the recent review literature [45–47].

3. Bayesian model parameter estimation

The multimodel inference process discussed in the previous section identifies a set of candidate model forms and their associated probabilities. For each of these models $M_j \in \mathcal{M}$ there are, of course, additional uncertainties associated with model parameters $\boldsymbol{\theta}_j$. These uncertainties are quantified using classical Bayesian inference applying Bayes' rule as

$$p(\boldsymbol{\theta}_j|\mathbf{d}, M_j) = \frac{p(\mathbf{d}|\boldsymbol{\theta}_j, M_j)p(\boldsymbol{\theta}_j|M_j)}{p(\mathbf{d}|M_j)} \propto p(\mathbf{d}|\boldsymbol{\theta}_j, M_j)p(\boldsymbol{\theta}_j|M_j), \quad j = 1, \dots, m \quad (13)$$

where, again, $p(\mathbf{d}|\boldsymbol{\theta}_j, M_j)$ is the likelihood function and $p(\boldsymbol{\theta}_j|M_j)$ is the prior probability density. The evidence, $p(\mathbf{d}|M_j)$, (Eq. (3)) serves only as a normalizing constant in this case. Therefore, unlike in the model selection process, it does not need to be evaluated explicitly as the posterior $p(\boldsymbol{\theta}_j|\mathbf{d}, M_j)$ can be estimated from samples using MCMC.

The simplest and most commonly used MCMC algorithms are Metropolis–Hastings (MH) [48] and Gibbs sampling [49]. In this work, we use an MH-based MCMC algorithm — the *Affine-invariant ensemble sampler* [50] proposed by Goodman and Weare [50] and implemented in the emcee software package [51]. The main advantage of this algorithm is that it leverages an ensemble of chains to adapt the proposal density through an implicit affine transformation. This has the effect of greatly improving efficiency for anisotropic and degenerate densities (increasing the acceptance rate while maintaining sample quality) and significantly reducing the correlation length of the Markov chains yielding independent samples more rapidly. An added benefit is that the method is largely “self-tuning” — requiring only one or two tuning parameters compared with $\sim N^2$ tuning parameters for most MH-based algorithms. For brevity, the reader is referred to [50,51] for algorithm details.

Although the parameter estimation performed here is conventional (nothing new), an important distinction of the multimodel parameter estimation process used herein is that we retain, and propagate, the full joint parameter density. Other conventional methods typically select a single, maximum likelihood parameter value and retain only the corresponding distribution for uncertainty propagation. This has the effect of ignoring parametric uncertainty. In combination with the multimodel selection, the result of our UQ process is therefore a set of probability models \mathcal{M} (with associated probabilities $\hat{\pi}_j$, $j = 1, \dots, m$), each of which has an associated joint parameter pdf $p(\boldsymbol{\theta}_j|\mathbf{d}, M_j)$. A method for propagation of this complete uncertainty has been previously proposed by the authors [23] and is reviewed in the following section.

4. Efficient multimodel uncertainty propagation

Given a set of probability models $\mathcal{M} = \{M_j\}$; $j = 1, \dots, m$ with posterior model probabilities $\hat{\pi}_j$ and joint posterior parameter densities $p(\boldsymbol{\theta}_j|\mathbf{d}, M_j)$, uncertainties associated with the random variable X are propagated using a Monte Carlo approach that employs importance sampling reweighting to reduce a nested Monte Carlo analysis to a single Monte Carlo analysis. More specifically, consider that X is now the input to some stochastic system $U = g(X)$. Given uncertainties in the form of the probability model of X (represented by the posterior model probabilities $\hat{\pi}_j$) and uncertainty in the parameters of each candidate model (described by the joint posterior parameter densities $p(\boldsymbol{\theta}_j|\mathbf{d}, M_j)$), we aim to quantify uncertainties in the response quantity U .

Conventional approaches to solving this type of problem involving uncertain probability distributions require nested Monte Carlo simulations where first the probability model space is sampled. That is, N_d probability models

are sampled from the multimodel set according to their associated model probability masses $\hat{\pi}_j$. For each of the N_d model-form samples, the parameter vector $\boldsymbol{\theta}_j$ is randomly sampled from the joint parameter pdf $p(\boldsymbol{\theta}_j|\mathbf{d}, M_j)$ to obtain a sample pdf (i.e. a realization of a specific model-form and its associated parameters). The set of N_d sample pdfs serves as a finite-dimensional approximation of the total uncertainty (both model-form and parametric) that can be propagated by Monte Carlo simulation. This is achieved by drawing N_s samples from each of the N_d distributions and evaluating the model $N_d \times N_s$ times. Clearly this is a highly inefficient process and is intractable for problems of even moderate computational expense.

The method proposed in [23] reduces this expense considerably to a single-loop Monte Carlo by employing importance sampling reweighting (also used in [6] for propagation of random sets). First, an optimal sampling density is identified by minimizing the expected mean square differences between the sampling density $q(\mathbf{x})$ and the ensemble of N_d probability models $p_i(\mathbf{x}|\boldsymbol{\theta}_i)$, $i = 1, \dots, N_d$. This corresponds to solving the following optimization problem under isoperimetric constraint $\hat{I}(q)$

$$\begin{aligned} & \underset{q}{\text{minimize}} \quad \hat{T}(q) = E_{\boldsymbol{\theta}} \left[\int_{\Omega} \hat{F}(\mathbf{x}, \boldsymbol{\theta}, q(\mathbf{x})) d\mathbf{x} \right] \\ & \text{subject to} \quad \hat{I}(q) = \int_{\Omega} q(\mathbf{x}) d\mathbf{x} - 1 = 0 \end{aligned} \quad (14)$$

where the action functional \hat{F} is the total square differences:

$$\hat{F}(\mathbf{x}, \boldsymbol{\theta}, q(\mathbf{x})) = \frac{1}{2} \sum_{i=1}^{N_d} (p_i(\mathbf{x}|\boldsymbol{\theta}_i) - q(\mathbf{x}))^2 \quad (15)$$

and $E_{\boldsymbol{\theta}}$ is the expectation with respect to the posterior probability of the model parameters $\boldsymbol{\theta}$. $\hat{I}(q)$ ensures that $q(\mathbf{x})$ is a valid pdf. It is shown that the optimization problem in Eq. (14) has closed-form solution given by the mixture model [23]

$$\hat{q}(\mathbf{x}) = \frac{1}{N_d} \sum_{i=1}^{N_d} E_{\boldsymbol{\theta}} [p_i(\mathbf{x}|\boldsymbol{\theta})]. \quad (16)$$

It is straightforward to show that this solution generalizes as:

$$\hat{q}(\mathbf{x}) = \sum_{i=1}^{N_d} \hat{\pi}_i E_{\boldsymbol{\theta}} [p_i(\mathbf{x}|\boldsymbol{\theta})] \quad (17)$$

where $\hat{\pi}_i$ is the posterior model probability for model M_i .

Samples are drawn from the optimal sampling density $\hat{q}(\mathbf{x})$ and the response of the system $g(\mathbf{x})$ evaluated at each sample point. The statistical response of the system $g(\mathbf{x})$ is reweighted according to each of the N_d sample pdfs using importance sampling as

$$E_q \left[g(\mathbf{x}) \frac{p(\mathbf{x})}{q(\mathbf{x})} \right] = \int_{\Omega} g(\mathbf{x}) \frac{p(\mathbf{x})}{q(\mathbf{x})} q(\mathbf{x}) d\mathbf{x} \approx \frac{1}{N} \sum_{i=1}^N g(\mathbf{x}_i) \frac{p(\mathbf{x}_i)}{q(\mathbf{x}_i)}. \quad (18)$$

The result is simultaneous propagation of all N_d probability models in the sampled set.

It is shown that this approach may be easily updated to accommodate new information from Bayesian inference as additional data are collected. This will typically reduce the uncertainty associated with the model form and parameters but will come at cost of a loss of optimality in the importance sampling density. If the change in optimal sampling density is considerable, the effect will be an increase in the statistical variance, or potential instability, of the importance sampling estimate. This can be addressed by resampling from the new optimal sampling density, but this is computationally prohibitive. In a forthcoming work [52], a method is proposed to efficiently accommodate a measure change in Monte Carlo simulation that minimizes the impact on the sample set. In other words, it retains as many samples as possible from the original Monte Carlo set drawn from density $\hat{q}(\mathbf{x})$ and adds a minimal number of samples from a “correction” density such that the combined set follows the desired new density $\hat{q}^*(\mathbf{x})$ while keeping the sample size constant. The method is utilized herein to maintain efficiency as data are added but, because it is not essential to the objective of this work (investigation of the effect of priors), the details are not included. The interested reader is referred to [52].

5. Formulating model and parameter priors

For a given set of models \mathcal{M} , the effectiveness of the Bayesian method depends firmly on the specification of the prior model probability $p(M_j)$ and the parameter prior $p(\boldsymbol{\theta}_j|M_j)$. Reasonable choices of prior distributions will have minor effects on posterior inference with well-identified parameters and large data size. However, when datasets are small and/or prior data is not entirely appropriate, specification of prior probabilities becomes very important. In this section, we briefly review approaches for formulating non-informative and data-driven, informative priors for multimodel inference.

5.1. Prior model probabilities

A popular and simple choice for the prior model probability $p(M_j)$, $j = 1, \dots, m$, is the uniform prior

$$\pi_j = p(M_j) = 1/m. \quad (19)$$

This prior is noninformative in the sense of favoring all models equally. Under this prior, the posterior model probability is equal to the ratio of the model evidence to the cumulative evidence,

$$\hat{\pi}_j = p(M_j|\mathbf{d}) = \frac{p(\mathbf{d}|M_j)}{\sum_{k=1}^m p(\mathbf{d}|M_k)} \quad (20)$$

and, as mentioned, these asymptotically correspond to the BIC model weights. However, the apparent noninformativeness of Eq. (20) can be deceptive since it is only uniform in probability and will typically not be uniform on the model characteristics. Hence, in setups where several models are very similar and only a few are different, Eq. (20) may bias the posterior model probability away from accurate models [53].

Burnham and Anderson [40] make a compelling case that model prior probabilities should depend on dataset size (n) and model complexity (i.e. number of model parameters, K_j). In other words, small datasets should have priors that favor less complex (lower-dimensional) models to avoid overfitting. This is a major motivation for the use of AIC as a model selection criterion given that it implies the use of savvy priors as discussed in Section 2.2. But, this effect is expected to be of minimal importance here as all of the considered probability models have comparable complexity.

Finally, model prior probabilities in real-world applications are often selected according to subjective preference, which may result from historical data, the modeler's experience, or solicited expert opinion. This is especially important as it will be shown that strong prior beliefs can greatly influence posterior model probabilities leading to very accurate (if the priors are correct) or inaccurate (if the priors are incorrect) assessments of uncertainty.

In this work, we consider each of these respective prior model probabilities and aim to understand their influence on uncertainty quantification and propagation.

5.2. Parameter prior probabilities

Prior probabilities for model parameters also play an important role in multimodel uncertainty quantification and propagation. Here, we broadly distinguish between so-called noninformative and informative priors and elaborate how these various priors can be constructed under conditions of ignorance (no prior information is available), previously existing (often historical) data, and under subjective assumptions.

5.2.1. Noninformative priors

One of the most common noninformative priors is the uniform prior that is flat, diffuse and often considered as “vague”. It is worth noting that a diffuse or vague prior may not be uniform and sometimes a diffuse prior can be more informative than the uniform prior [54–56]. The uniform prior can be expressed as

$$p(\boldsymbol{\theta}_j|M_j) = \text{Constant}, \quad \boldsymbol{\theta}_j \in \Omega_{\theta_j} \quad 1 \leq j \leq m \quad (21)$$

where the range of $\boldsymbol{\theta}_j$, Ω_{θ_j} is a subset of the parameter space $\boldsymbol{\theta}_j$ ($\Omega_{\theta_j} \subset \boldsymbol{\theta}_j$). This indicates that there is no *a priori* reason to favor any particular parameter value. Instead, we only know its range $\boldsymbol{\theta}_j \in \Omega_{\theta_j}$. Thus, the posterior distribution in Eq. (13) is proportional to the likelihood,

$$p(\boldsymbol{\theta}_j|\mathbf{d}, M_j) \propto p(\mathbf{d}|\boldsymbol{\theta}_j, M_j), \quad \boldsymbol{\theta}_j \in \Omega_{\theta_j} \quad 1 \leq j \leq m. \quad (22)$$

If the range Ω_{θ_j} is specified as the parameter space $\Omega_{\theta_j} = \Theta_j$, Bayesian inference assuming a flat prior may cause an improper prior if

$$\int_{\Theta_j} p(\boldsymbol{\theta}_j | M_j) d\boldsymbol{\theta}_j = \infty, \quad 1 \leq j \leq m. \quad (23)$$

In this case the normalizing constant sometimes does not exist. If an improper prior is employed, one needs to be sure that the posterior is proper.

Another commonly used noninformative prior is the Jeffreys prior [57], which is defined to be proportional to the square root of the determinant of the Fisher information matrix

$$p(\boldsymbol{\theta}_j | \mathbf{d}, M_j) \propto |J(\boldsymbol{\theta}_j)|^{1/2}, \quad 1 \leq j \leq m. \quad (24)$$

The Fisher information is given as:

$$J(\boldsymbol{\theta}_j) = - \int E \left[\frac{\partial^2 \log p(\mathbf{x} | \boldsymbol{\theta}_j, M_j)}{\partial \boldsymbol{\theta}_j \partial \boldsymbol{\theta}_j^T} \right] p(\mathbf{x} | \boldsymbol{\theta}_j, M_j) d\mathbf{x}, \quad 1 \leq j \leq m. \quad (25)$$

For certain models, the Jeffreys prior cannot be normalized and is therefore an improper prior in such cases.

In this work, we employ proper uniform priors as representative noninformative priors. While this admittedly does not account for various nuances that may arise from assuming different noninformative priors, the intention here is to compare the effects of a suitably representative noninformative prior on multimodel uncertainty quantification and propagation against the effects of various informative priors.

5.2.2. Informative priors

At the other extreme, an informative prior is one that yields a posterior that is not dominated by the likelihood; instead an informative prior has an essential impact on the posterior distribution. This is especially true for inference from small datasets. The appropriate use of informative priors illustrates the power of the Bayesian approach: information gathered from previous studies, past experiences or expert opinions can be combined with new data in a natural way. We can therefore interpret an informative prior as the state of our subjective prior knowledge. However, in practice, prior specification of subjective knowledge might be biased as it is often difficult to specify precisely and historical data, experiments, and experiences may not be totally appropriate for the current problem. One objective of this study is to understand the influence of such imprecise and/or incorrect informative priors on multimodel uncertainty quantification and propagation.

In this work, we formulate data-driven informative priors by exploiting historical data, denoted $\hat{\mathbf{d}}$, as may be available in the literature. We specifically avoid formulating priors based on assumptions or intuition. In this sense, the historical data $\hat{\mathbf{d}}$ represents the existing state of knowledge as objectively as possible. Yet, as previously mentioned, these data may not be entirely appropriate for the problem at hand and therefore may or may not provide “good” priors.

The data-driven prior is quantified by applying Bayes’ rule to the historical data, $\hat{\mathbf{d}}$. The posterior then becomes the prior for the analysis using the currently observed data, \mathbf{d} . This initial Bayesian inference starts with a suitable noninformative prior, termed the “pre-prior”. Within this framework, the currently observed data \mathbf{d} is effectively treated as an extension of the historical data $\hat{\mathbf{d}}$. If the historical dataset is relatively large, the resulting prior is referred to as strongly informative and dominates the pre-prior. If the historical dataset is small, the resulting prior is referred to as weakly informative and retains some influence of the noninformative pre-prior.

The approach used in this work is summarized in three stages as follows:

- *Stage 1: Noninformative pre-prior* — Noninformative pre-priors $\hat{p}(\boldsymbol{\theta}_j | M_j)$ can be developed in a number of different ways. When the likelihood function $\hat{p}(\hat{\mathbf{d}} | \boldsymbol{\theta}_j, M_j)$ is given, one can derive the noninformative prior based on Jeffrey’s rule, or simply use a flat prior instead.
- *Stage 2: Pre-Bayesian inference* — A pre-Bayesian inference is employed herein to identify the posterior distribution based on historical data $\hat{\mathbf{d}}$ combined with a given noninformative prior $\hat{p}(\boldsymbol{\theta}_j | M_j)$ and the specified model M_j

$$p^*(\boldsymbol{\theta}_j | M_j) = \hat{p}(\boldsymbol{\theta}_j | \hat{\mathbf{d}}, M_j) = \frac{\hat{p}(\hat{\mathbf{d}} | \boldsymbol{\theta}_j, M_j) \hat{p}(\boldsymbol{\theta}_j | M_j)}{\int_{\Theta_j} \hat{p}(\hat{\mathbf{d}} | \boldsymbol{\theta}_j, M_j) \hat{p}(\boldsymbol{\theta}_j | M_j) d\boldsymbol{\theta}_j}, \quad 1 \leq j \leq m. \quad (26)$$

The posterior distribution $\hat{p}(\boldsymbol{\theta}_j | \hat{\mathbf{d}}, M_j)$ is taken as the prior distribution $p^*(\boldsymbol{\theta}_j | M_j)$ for the currently observed data \mathbf{d} .

- *Stage 3: Nonparametric estimate from posterior samples* — Eq. (26) is typically solved implicitly using MCMC. Therefore, the data-driven prior is not available in closed-form for Bayesian updating using the new data, \mathbf{d} . A nonparametric kernel density estimate is therefore used to approximate the unknown prior probability density function from the MCMC samples.

For multivariate density functions involving parameter vector $\boldsymbol{\theta}_j$ with dimension K_j , the kernel density estimate $\tilde{f}(\boldsymbol{\theta}_j | M_j)$ has the form given a sample set $\boldsymbol{\theta}_j = \{\boldsymbol{\theta}_j^1, \boldsymbol{\theta}_j^2, \dots, \boldsymbol{\theta}_j^n\}$ of size n given model M_j [58] as

$$\tilde{f}(\boldsymbol{\theta}_j | M_j) = \frac{1}{n} \sum_{k=1}^n \prod_{i=1}^{K_j} \left\{ \frac{1}{w_i} \phi \left(\frac{\boldsymbol{\theta}_{j,i} - \boldsymbol{\theta}_{j,i}^k}{w_i} \right) \right\}, \quad 1 \leq j \leq m \quad (27)$$

where $\boldsymbol{\theta}_{j,i}^k$ is the k th sample in the i th dimension of $\boldsymbol{\theta}_j$ given model M_j , and w_i the corresponding bandwidth. $\phi(\cdot)$ is a chosen Gaussian kernel given by

$$\phi(x) = \frac{1}{\sqrt{2\pi}} e^{-x^2/2}. \quad (28)$$

The kernel bandwidth is then determined by minimizing the asymptotic mean integrated square error (AMISE) [59] such that, for the Gaussian kernel, the optimal bandwidth is

$$w_i^{opt} = \left[\frac{4}{K_j + 2} \right]^{1/(K_j+4)} n^{-1/(K_j+4)} \sigma_i \quad (29)$$

where σ_i is the standard deviation of the samples $\{\boldsymbol{\theta}_{j,i}^1, \boldsymbol{\theta}_{j,i}^2, \dots, \boldsymbol{\theta}_{j,i}^n\}$. The kernel density estimate $\tilde{f}(\boldsymbol{\theta}_j | M_j)$ is then employed as the informative prior for Bayesian inference using the observed data \mathbf{d} .

6. Application: plate buckling strength problem

Uncertainty in the material and geometric properties of ship structural components can significantly impact the performance, reliability and safety of the structural system [60]. In this work, we apply the proposed methodology to quantify and propagate the uncertainty in material properties for buckling strength of a simply supported rectangular plate under uniaxial compression. An analytical formulation for the normalized buckling strength for a pristine plate was first proposed by Faulkner [61]

$$\psi = \frac{\sigma_u}{\sigma_0} = \frac{2}{\lambda} - \frac{1}{\lambda^2} \quad (30)$$

where σ_u is the ultimate stress at failure, σ_0 is the yield stress, and λ is the slenderness of the plate with width b , thickness t , and elastic modulus E given by

$$\lambda = \frac{b}{t} \sqrt{\frac{\sigma_0}{E}}. \quad (31)$$

Eq. (31) was further modified by Carlsen [62] to study the effect of residual stresses and non-dimensional initial deflections δ_0 associated with welding

$$\psi = \left(\frac{2.1}{\lambda} - \frac{0.9}{\lambda^2} \right) \left(1 - \frac{0.75\delta_0}{\lambda} \right) \left(1 - \frac{2\eta t}{b} \right) \quad (32)$$

where ηt is the width of the zone of tension residual stress.

The design buckling strength is based on nominal values for the six variables in Eq. (32) provided in Table 1. However, the actual values of these variables often differ from the design values due to uncertainties in the material properties and “as built” geometry yielding uncertainty in the buckling strength. We are therefore interested in investigating the effect of the six uncertain variables shown in Table 1 on the buckling strength of simply supported mild steel plates. Emphasis is placed on assessing the influence of uncertainty in the yield strength σ_0 since it is the most sensitive variable identified by Global sensitivity analysis (see Table 1) and for clarity of demonstration.

Table 1

Statistical properties of plate material, geometry and imperfection variables from Hess et al. [63] and Guedes Soares [64].

Variables	Physical meaning	Nominal value	Mean	COV	Global sensitivity
b	Width	36	0.992 * 36	0.028	0.017
t	Thickness	0.75	1.05 * 0.75	0.044	0.045
σ_0	Yield strength	34	1.023 * 34	0.116	0.482
E	Young's modulus	29 000	0.987 * 29 000	0.076	0.194
δ_0	Initial deflection	0.35	1.0 * 0.35	0.05	0.043
η	Residual stress	5.25	1.0 * 5.25	0.07	0.233

Table 2

Statistical information and comments of informative knowledge from historical data.

Steel type	Min	Max	Mean	COV	Distribution	# of tests	Comments
ABS-A	31.9	39.6	36.091	0.059	Lognormal	33	Weakly informative but incorrect
ABS-B	27.6	46.8	34.782	0.116	Lognormal	79	Informative and correct
ABS-C	30.9	41.5	33.831	0.081	Lognormal	13	Weakly informative but incorrect
ASTM-A7	28.6	49.4	38.197	0.108	Normal	58	Informative but incorrect

6.1. Description of historical data

The work of Hess et al. [63] presented a review of uncertainties in material and geometric properties for mild steel plates for ship building applications. They conducted statistical analysis of data compiled from tests/measurements sponsored by the Ship Structure Committee (SSC) [65,66] as part of an effort to establish a database of marine steel properties and tests/measurements performed by the Naval Surface Warfare Center, Carderock Division (NSWCCD). These past sources of yield strength data are very important because they provide a valuable source of prior information. However, it remains difficult to represent the uncertainties since the measured data are scarce. Hence, quantification of uncertainties and variations is necessary to determine the probabilistic characteristics of these random variables. In this work, we make use of the historical experimental data to predict the probabilistic characteristics of yield strength of mild steel. The source of the material property data is a series of historical reports from the SSC-352 [67], SSC-142 [68] and SSC-145 [69], which include material from four classes of structural steels summarized as follows

- ABS-A — plates with thickness not exceeding 1/2 inch and all shapes
- ABS-B — plates with thickness over 1/2 inch but not exceeding 1 inch
- ABS-C — plates with thickness over 1 inch
- ASTM-A7 — historical conventional structural steel alloy replaced by ASTM-A36.

The three ABS steels are typical ship-building and marine steels and vary somewhat in chemical composition but possess nominally the same design properties (most notably $\sigma_0 = 34$ ksi) while the ASTM-A7 is a historical carbon steel having design yield strength in the range $\sigma_0 = [30, 33]$ ksi. The statistical analysis of these data are reproduced from Hess et al. [63] in Table 2. These data are useful for our purposes since they are representative of the type of historical data (these tests date back to 1948) that may be available for assigning prior distributions in Bayesian inference but are not truly representative of what may be expected from modern materials. Thus, the statistical analysis of the four materials provided by [63] gives us different priors from which to initiate our investigation.

The application of interest here is a ship structural plate with thickness $t = 0.75$ inch. It is therefore of ABS-B material class and we assume that the “true” model for the ABS-B material is that given in Table 2. Note that, in reality, this is not in fact the true model for ABS-B material but for our purposes it provides a baseline from which we have an *informative* and *correct* prior. The ABS-A and ABS-C materials are similar to the “true” ABS-B material and their datasets smaller so are considered to provide weakly informative but technically incorrect priors. Finally, the ASTM-A7 material is considerably different. Given that it is a comparatively large dataset, we consider it to give an informative but incorrect prior. Note that, under practical conditions of limited data, an analyst may consider any one of these datasets to be “close enough” so as to define a prior for UQ (justifiably or not). Our objective is to study the influence of using these different priors in the context of multimodel Bayesian UQ.

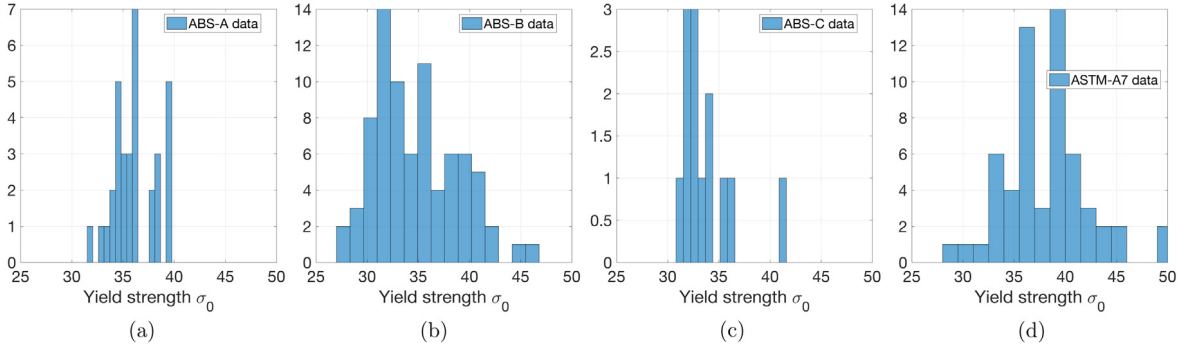


Fig. 1. Histograms of material data for (a) ABS-A, (b) ABS-B, (c) ABS-C and (d) ASTM-A7.

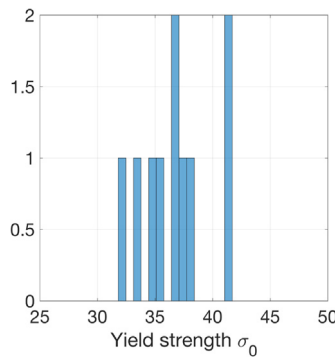


Fig. 2. Ten randomly sampled yield strength data that serve as the initial dataset.

Fig. 1 shows histograms of the material data for each of the four classes: ABS-A, ABS-B, ABS-C and ASTM-A7. The ABS-B material data collected from the technical report SSC-142 [68] has mean $\mu = 34.782$, coefficient of variation 0.116, and is assumed to follow a lognormal distribution. Again, we assume this to be the “true” model and, for our investigation, all “data” are synthetically generated from $\sigma_0 \sim \text{Lognormal}(\mu_{\sigma_0} = 34.782, \sigma_{\sigma_0} = 0.116 * 34.782)$. The initial 10 yield strength values are shown in **Fig. 2**. Given these 10 values and the prior data, we contend that a single probability model form cannot be precisely identified. Therefore, we select seven candidate probability models including Gamma, Inverse Gaussian, Logistic, Loglogistic, Lognormal, Normal and Weibull. For each of these models, prior parameter densities are derived from each dataset in **Fig. 1** as described in Section 5.2.2 and Bayesian inference performed in the following.

6.2. Influence of data-driven priors on uncertainty quantification

In multimodel Bayesian UQ, there are two stages of inference related to model-form uncertainty (Section 2) and model parameter uncertainty (Section 3). There is an interesting interplay between these two stages of inference as suggested by Eqs. (2)–(3) and the flowchart in **Fig. 3**. In the first stage, multiple candidate models are considered (i.e. the seven model listed above) and some assumptions are made regarding their prior model probabilities — perhaps informed by expert opinion. As data are collected, the model probabilities are updated using Bayes’ rule (Eqs. (2)–(3)). But, these updated probabilities are influenced by the selection of the parameter prior in Eq. (3) and, as we will see, this can play an important role in model selection. In the second stage, the model parameter distributions are inferred from the data for each model form. These are obviously strongly dependent on the prior parameter densities. These inference processes combine to provide the posterior information used to quantify uncertainty in the parameter of interest (here σ_0). Sections 6.2.1 and 6.2.2 aim to answer the question: What influence does prior assumptions (in model-form and model parameters) have on the accuracy and convergence of posterior probabilities?

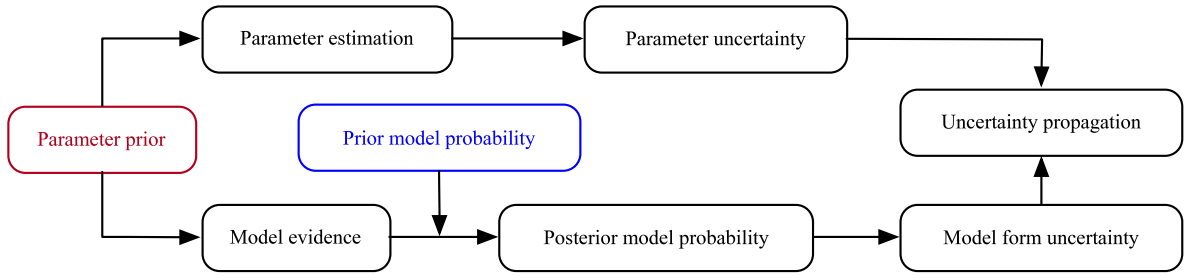


Fig. 3. Influence of parameter prior and model prior probability on uncertainty quantification and propagation.

Table 3

Prior model probabilities.

	Uniform	“Strong correct”	“Strong incorrect”
Gamma	1/7	0.0167	0.0167
Inverse Gaussian	1/7	0.0167	0.0167
Logistic	1/7	0.0167	0.0167
Log-logistic	1/7	0.0167	0.9
Lognormal	1/7	0.9	0.0167
Normal	1/7	0.0167	0.0167
Weibull	1/7	0.0167	0.0167

6.2.1. Effect of priors on model-form uncertainty

In Bayesian model selection, it is common to assume equal prior probability (i.e. $\pi_j = P(M_j) = 1/m = 1/7$) [53]. In certain instances, subjective non-equal probabilities may be assigned. In fact, for our problem the existing literature suggests a “preferred” distribution for σ_0 (Hess et al. [63] suggest a lognormal distribution). With this information, we assign a prior model probability $\pi_{LN} = 0.9$ and assume equal weight ($\pi_j = \frac{1-0.9}{6}$, $j \neq LN$) for the other models. Because there is a strong belief in the correct prior model, we refer to this as the “strong correct” prior. This strong correct prior will be compared against the uniform prior of equal probabilities as well as a “strong incorrect” prior wherein there is strong belief in the incorrect log-logistic model such that it has prior probability $\pi_{LL} = 0.9$ and all other prior probabilities are equal. The three model prior cases we consider are summarized in Table 3.

As data are collected, posterior model probabilities are updated according to Eqs. (2)–(3). These probabilities depend on the parameter prior assumption and, as a result, they will differ based on the historical data we use to derive the prior. In the small data case, it can be quite difficult to make any meaningful conclusions regarding model probabilities as evidenced by the data in Table 4, which gives the posterior model probabilities from 10 yield stress data for each of the parameter priors given equal prior model probabilities. Note that in these cases, the posterior is simply equal to the model evidence. This is a classic small data case where a precise “best” model is impossible to identify. Moreover, as suggested by the definition of model evidence, these posterior model probabilities are strongly dependent on the parameter prior with considerable differences across different priors.

We are also interested in the convergence of the model-form uncertainty as a function of the amount of data collected. The previous discussion in Table 4 highlighted how very small datasets lead to large model-form uncertainties — with further uncertainty introduced by the selection of the parameter prior. But how much data is necessary to reduce this uncertainty and how does the performance change given different parameter priors? Fig. 4 shows the posterior model probabilities as a function of dataset size for different parameter priors (given equal prior model probabilities). For comparison, Fig. 5 shows the posterior model probabilities using AIC model selection (i.e. using savvy prior probabilities). Notice that the AIC, noninformative, and ABS-B priors show nearly identical trends with added data. Although they fail to identify a unique model (they essentially identify the lognormal and the inverse Gaussian with equal probability), we will see that they are in fact among the “best” priors in terms of convergence toward the true probability model. Of particular interest is the fact that the ABS-A parameter prior converges toward the incorrect Gamma model and effectively discounts the lognormal model entirely.

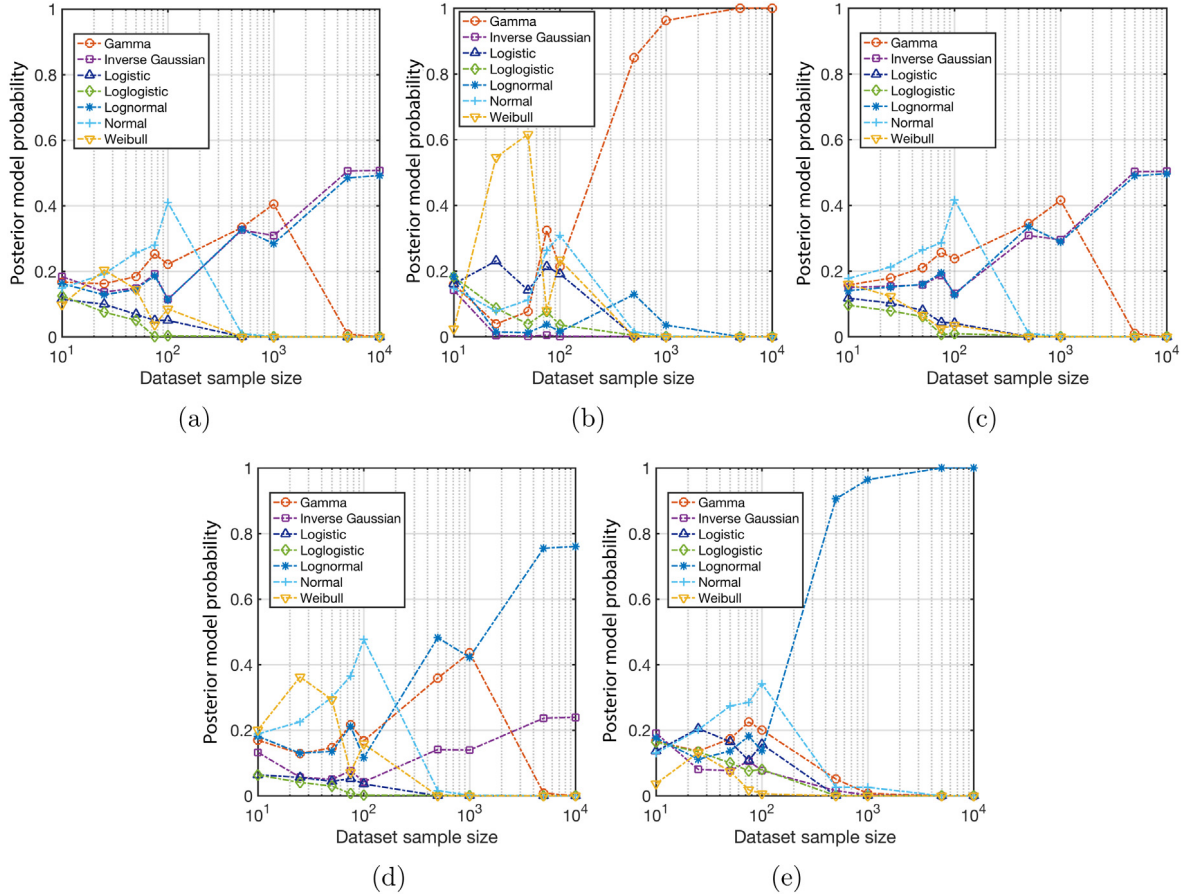


Fig. 4. Posterior model probabilities given equal prior model probabilities as a function of dataset size for different parameter priors: (a) Noninformative prior, (b) ABS-A prior, (c) ABS-B prior, (d) ABS-C prior and (e) ASTM-A7 prior.

Table 4

Posterior model probabilities given initial 10 data and different parameter priors.

Distribution	AIC	Noninformative	ABS-A	ABS-B	ABS-C	ASTM-A7
Gamma	0.168	0.167	0.159	0.157	0.170	0.166
Inverse Gaussian	0.172	0.184	0.142	0.150	0.132	0.191
Logistic	0.119	0.115	0.161	0.118	0.064	0.136
Loglogistic	0.128	0.125	0.182	0.096	0.063	0.163
Lognormal	0.167	0.162	0.184	0.140	0.182	0.176
Normal	0.154	0.149	0.147	0.178	0.189	0.130
Weibull	0.091	0.098	0.024	0.160	0.201	0.037

Use of informative model prior probabilities can change this convergence behavior considerably. Figs. 6 and 7 show the posterior model probabilities with dataset size for each of the seven models given the strong correct prior (Fig. 6) and the strong incorrect prior (Fig. 7) for each of the considered parameter priors.

For the strong correct model prior, four of the five cases show convergence toward the true lognormal model from which the data are drawn as the dataset grows large. Even with the strong incorrect model prior probabilities, the multimodel inference eventually suppresses the incorrect log-logistic model and identifies the correct lognormal form in these cases — indicating a degree of robustness for these parameter priors. Note also the ABS-B with strong incorrect prior yields essentially equally probable lognormal and inverse Gaussian models because, under this prior the distributions are nearly identical in shape and the inference cannot discern between them.

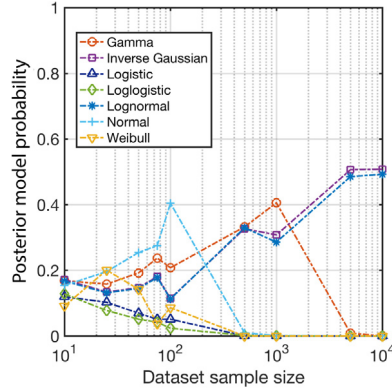


Fig. 5. Posterior model probabilities from AIC model selection.

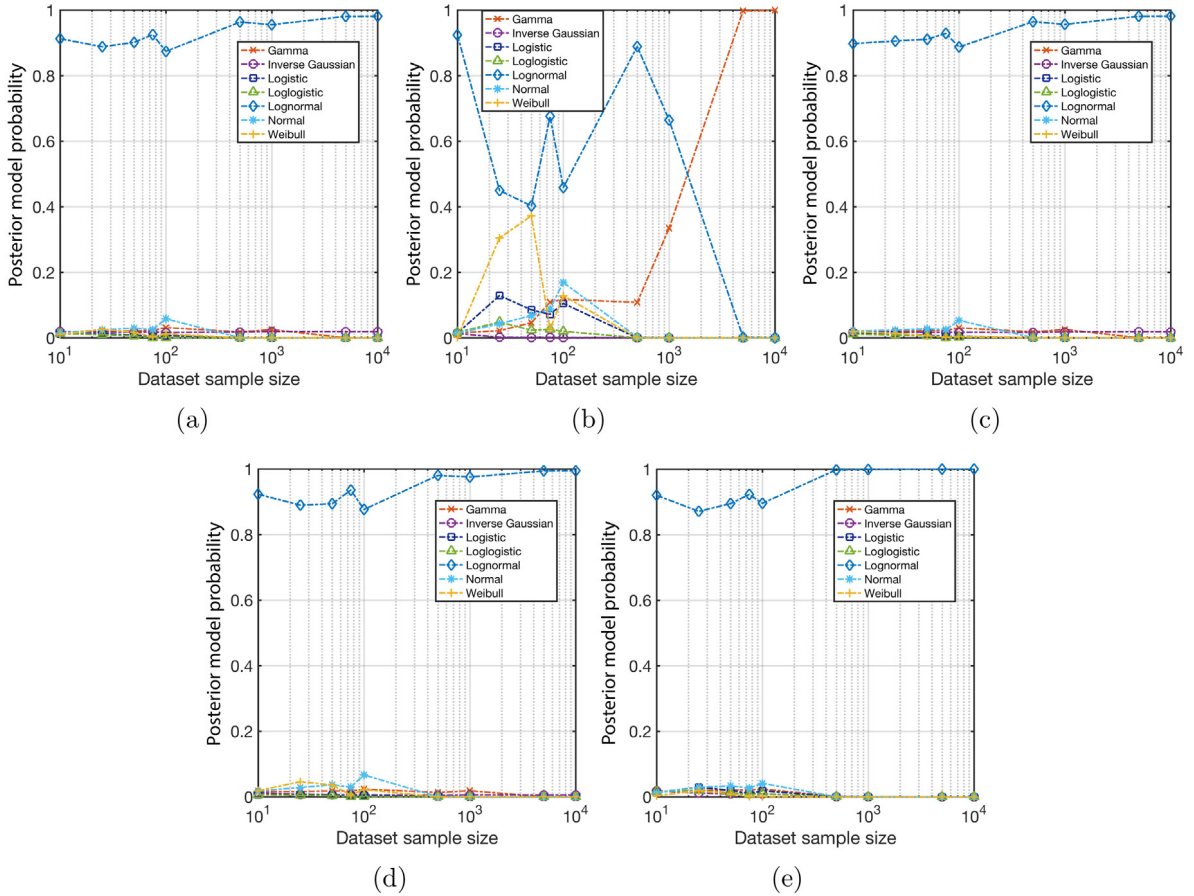


Fig. 6. Posterior model probabilities given “strong correct” prior model probabilities as a function of dataset size for different parameter priors:
(a) Noninformative prior, (b) ABS-A prior, (c) ABS-B prior, (d) ABS-C prior and (e) ASTM-A7 prior.

In both cases, the ABS-A parameter prior causes the inference to converge to the wrong Gamma model form even when 10,000 yield stress values are collected. The reason for this will be explored later but this points to the important conclusion that if the parameter prior is not wisely chosen, it may not be possible to infer even the correct model form for the data. This can have significant practical implications for uncertainty quantification and propagation.

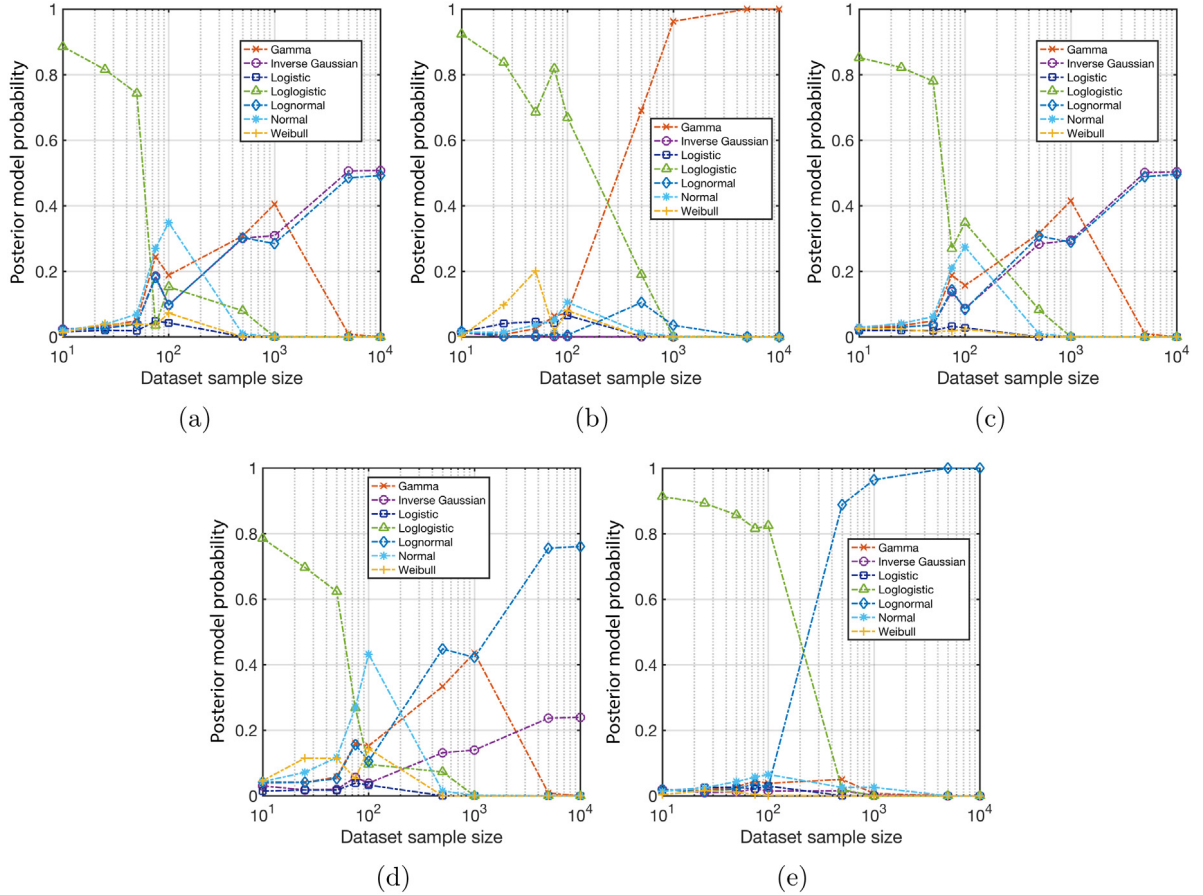


Fig. 7. Posterior model probabilities given “strong incorrect” prior model probabilities as a function of dataset size for different parameter priors: (a) Noninformative prior, (b) ABS-A prior, (c) ABS-B prior, (d) ABS-C prior and (e) ASTM-A7 prior.

6.2.2. Effect of parameter prior on parameter uncertainty

For each model form, the selection of the parameter prior will significantly impact the convergence of the posterior. Here, we focus on the case of the lognormal distribution as a representative case to illustrate this effect. Similar results for the other probability models were observed.

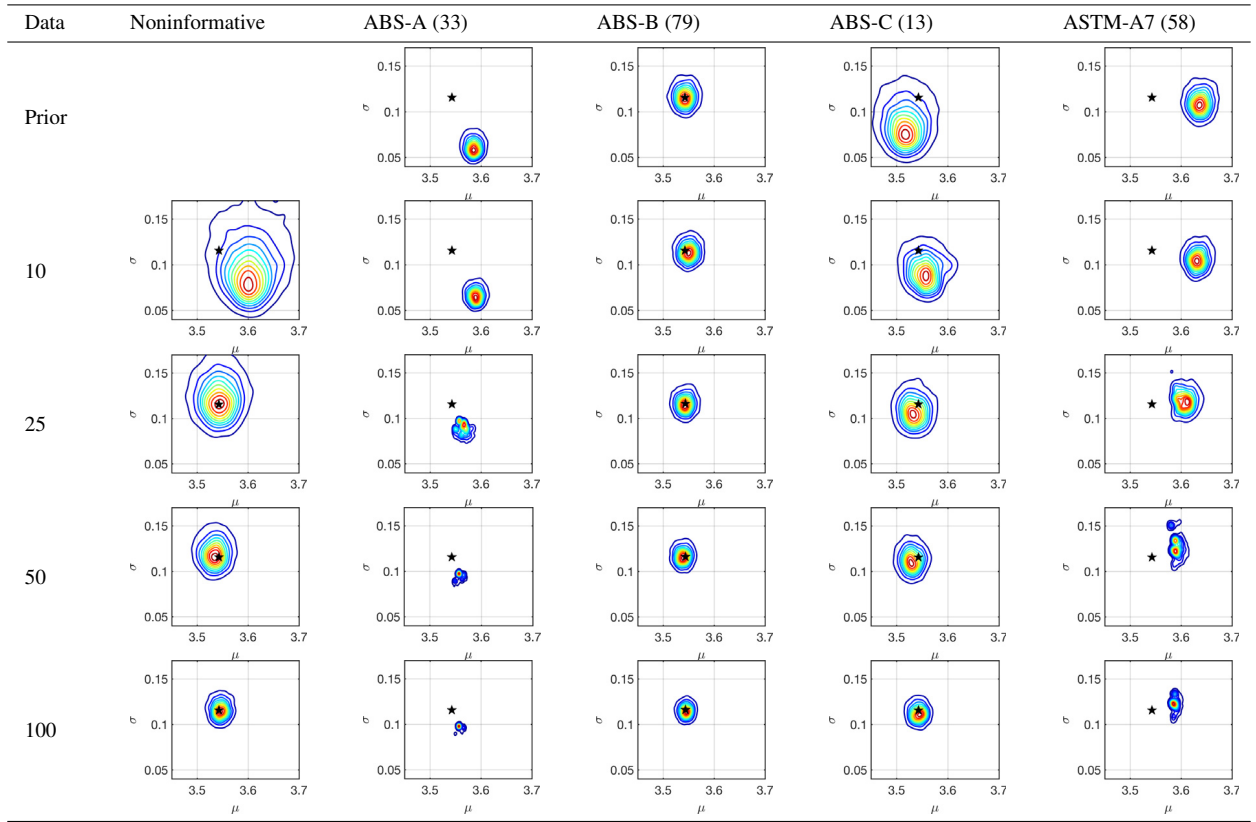
Data are generated according to the “true” lognormal distribution and Bayesian inference conducted to infer the parameters of the lognormal model using each of the five considered parameter priors. Table 5 shows the joint parameter pdf for “small” datasets (≤ 100 data) along with the true parameters (indicated by a \star). Notice that the ABS-A and ASTM-A7 priors yield the most rapid convergence but neither their priors nor their posteriors include the true parameter values. Indeed, these models are unable to infer the correct distribution despite the prior belief that they may serve as reasonable priors. The noninformative and ABS-C priors provide relatively similar levels of convergence and include the true model. This is because they are sufficiently weak in the amount of incorrect information they provide. Lastly, as expected the correct ABS-B prior exhibits the best convergence to the true model.

Table 6 provides similar plots for “large” datasets (≥ 500 data). We see that the models with ABS-A and ASTM-A7 priors continue to narrow and move slowly toward the correct parameters. However, even after 10,000 data are collected they do not come to include the correct parameters in their joint density with any significant probability. The noninformative, ABS-B, and ABS-C meanwhile continue to converge correctly at similar rates (there is very little improvement from using the ABS-B prior for large datasets).

An alternative way to look at this is to populate a set of possible distributions by Monte Carlo sampling from the joint parameter densities. This is useful both for illustration purposes and because, as shown in the following

Table 5

Posterior parameter joint probability densities for the lognormal distribution with different priors considering small dataset size (≤ 100 data).



section, we do this in order to propagate the total uncertainty. Table 7 shows how these distributions change with dataset size for the noninformative, ABS-B, and ABS-A parameter priors. Notice that the band of distributions for the noninformative and ABS-B priors includes the true distribution (bold) while the ABS-A case does not. Moreover, the band of distributions from the ABS-A prior is significantly narrower than those from both the noninformative and ABS-B priors, which implies confidence in the distribution. In other words, this prior gives false confidence in the wrong set of models. This may have major implications on uncertainty propagation, which is taken up in Section 6.3.

6.2.3. Effect of priors on total uncertainty

The total uncertainty in the yield strength is represented by Monte Carlo sampling from the candidate distributions as described in Section 4. For each sample (pdf), a probability model is randomly selected according to the posterior model probabilities. The parameters of this model are then randomly sampled from its posterior joint pdf. The result is a Monte Carlo set of distributions as shown in Fig. 8. This particular example shows a set of 5000 distributions given equal prior model probabilities with noninformative parameter priors for cases having datasets of size 10, 100, and 1000 data.

To measure the degree of uncertainty in a given model set, we compute the average mean square distance between the 5000 models in the set and the true lognormal density given by:

$$\delta = \frac{1}{2} \frac{1}{5000} \sum_{i=1}^{5000} (p_i(\mathbf{x}|\boldsymbol{\theta}) - p(\mathbf{x}))^2 \quad (33)$$

where $p_i(\mathbf{x}|\boldsymbol{\theta})$ are the distributions in the set and $p(\mathbf{x})$ is the lognormal pdf of the true model. This distance is plotted as a function of dataset size in Fig. 9 for each parameter prior and for the three cases of model prior probabilities. When the dataset size is small, there is a major benefit to using the correct ABS-B prior. That is, the set of distributions

Table 6

Posterior parameter joint probability densities for the lognormal distribution with different priors considering large dataset size (≥ 500 data).

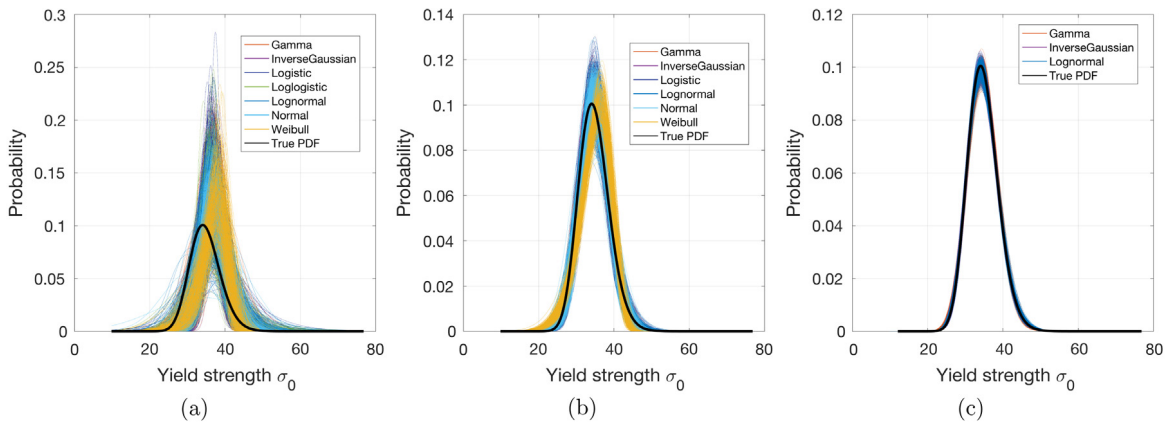
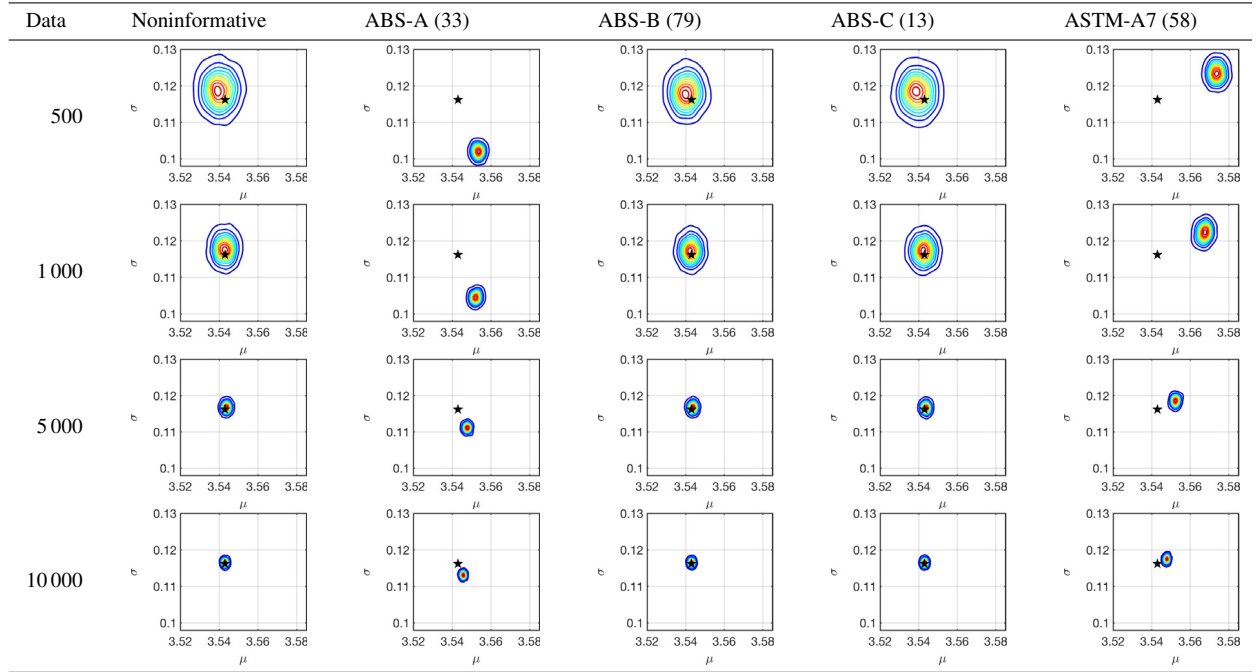


Fig. 8. 5000 distributions given equal model prior probabilities with noninformative parameter priors for (a) 10 data, (b) 100 data and (c) 1000 data.

is comparatively close to the true distribution. All other priors, meanwhile, start by poorly representing the true distribution (relatively large average mean square distance to the true distribution) but the noninformative and ABS-C priors come to be almost as good as the ABS-B prior after ~ 100 data are collected. The ABS-A and ASTM-A7 priors, on the other hand, cannot achieve the same level of accuracy as the other priors — even for very large datasets. The result is that the set of distributions generated from the ABS-A and ASTM-A7 priors can have residual errors that effectively result in identification/propagation of incorrect probability models (as evidenced again by the lognormal distributions from the ABS-A prior in Table 7 which do not include the true model).

Table 7

Monte Carlo sets of lognormal distributions drawn from the posterior parameter densities given noninformative, ABS-A, and ABS-B prior parameter densities.

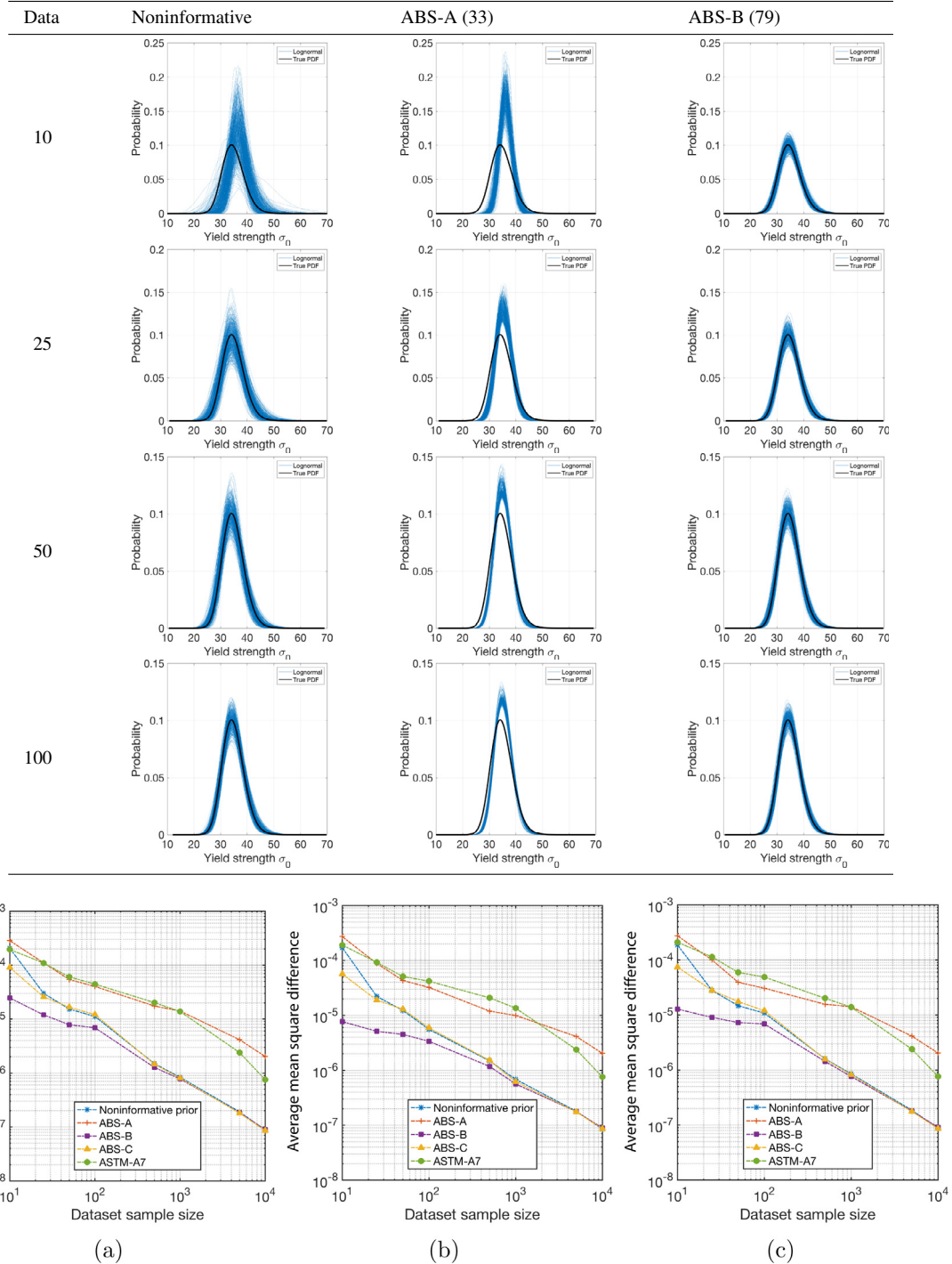


Fig. 9. Convergence of average mean square distance for (a) equal model prior, (b) strong correct model prior and (c) strong incorrect model prior.

6.3. Influence of data-driven priors on uncertainty propagation

The results of the multimodel inference process are used to identify a set of probability models (e.g. Fig. 8) that can be propagated through a physics-based model using the method in Section 4 [23]. Given the sensitivity of the posterior probabilities to the selection of the prior, this begs the question: What impact does prior assumptions have on response quantities from the model? If the prior yields rapid convergence, it stands to reason that we should expect rapid convergence (i.e. small uncertainty) in response quantities. But, how much of an improvement can be gained through good prior selection and how poor are the results if a bad prior is selected? The results of the previous section seem to imply that a poor prior can yield not just large uncertainties, but incorrect probabilistic response. We explore these issues in the context of our plate buckling problem in this section.

Total uncertainty is propagated using the IS reweighting method proposed in [23] and reviewed in Section 4. For illustration, consider quantification based on the ABS-B parameter prior with equal prior model probabilities. Table 8 shows the results of propagation for uncertainties quantified from different size datasets. The left column shows the set of 5000 probability densities identified from MC sampling of the quantified uncertainties in model form and parameters along with the optimal sampling density for propagation. The second column shows the set of CDFs for the buckling strength along with the true buckling strength CDF from propagating the true lognormal model. Notice that the true is fully encapsulated within the set of propagated distributions. The final columns show CDFs for the mean buckling strength and probability of failure ($P_f = P(\psi < 0.6)$). The bold line gives the overall CDF considering all model forms (and their probabilities) while the colored CDFs are conditional CDFs for each plausible model form. Also shown in these figures are the true mean buckling strength and P_f which, in all cases, fall within the range of the CDFs.

As expected, the uncertainty diminishes with increased dataset size. More specifically, the band of distributions in the input PDFs and output CDFs narrows toward their correct distributions. Also, the range of the CDFs for mean buckling strength and P_f narrow toward the true values as the dataset size increases.

These trends are clear and illustrate the method's performance for cases where a good prior (ABS-B) is selected. But, do these trends hold for other priors? To assess the effect of different priors, we quantify the convergence of the mean buckling strength, variance of buckling strength, and P_f using two different metrics. The first is a simple quantile confidence metric which defines the 95% confidence range for statistic Y given n data by:

$$\delta_Y^{(n)} = Q_{0.975}(Y^{(n)}) - Q_{0.025}(Y^{(n)}). \quad (34)$$

The ranges for the mean, variance, and P_f are therefore denoted $\delta_\mu^{(n)}$, $\delta_{\sigma^2}^{(n)}$, and $\delta_{(\psi < \psi^*)}^{(n)}$. The second is an accuracy metric, the “area validation metric” [70,71], that measures the difference in area between the CDF and the true value for statistic Y given n data as:

$$d_Y^{(n)}(F, T) = \int_{-\infty}^{\infty} |F(Y) - T(Y)| dy \quad (35)$$

where $F(Y)$ is the CDF from the simulation and $T(Y)$ is the true value. For the mean, variance, and P_f the accuracy metrics are therefore denoted by $d_\mu^{(n)}$, $d_{\sigma^2}^{(n)}$, and $d_{(\psi < \psi^*)}^{(n)}$, respectively.

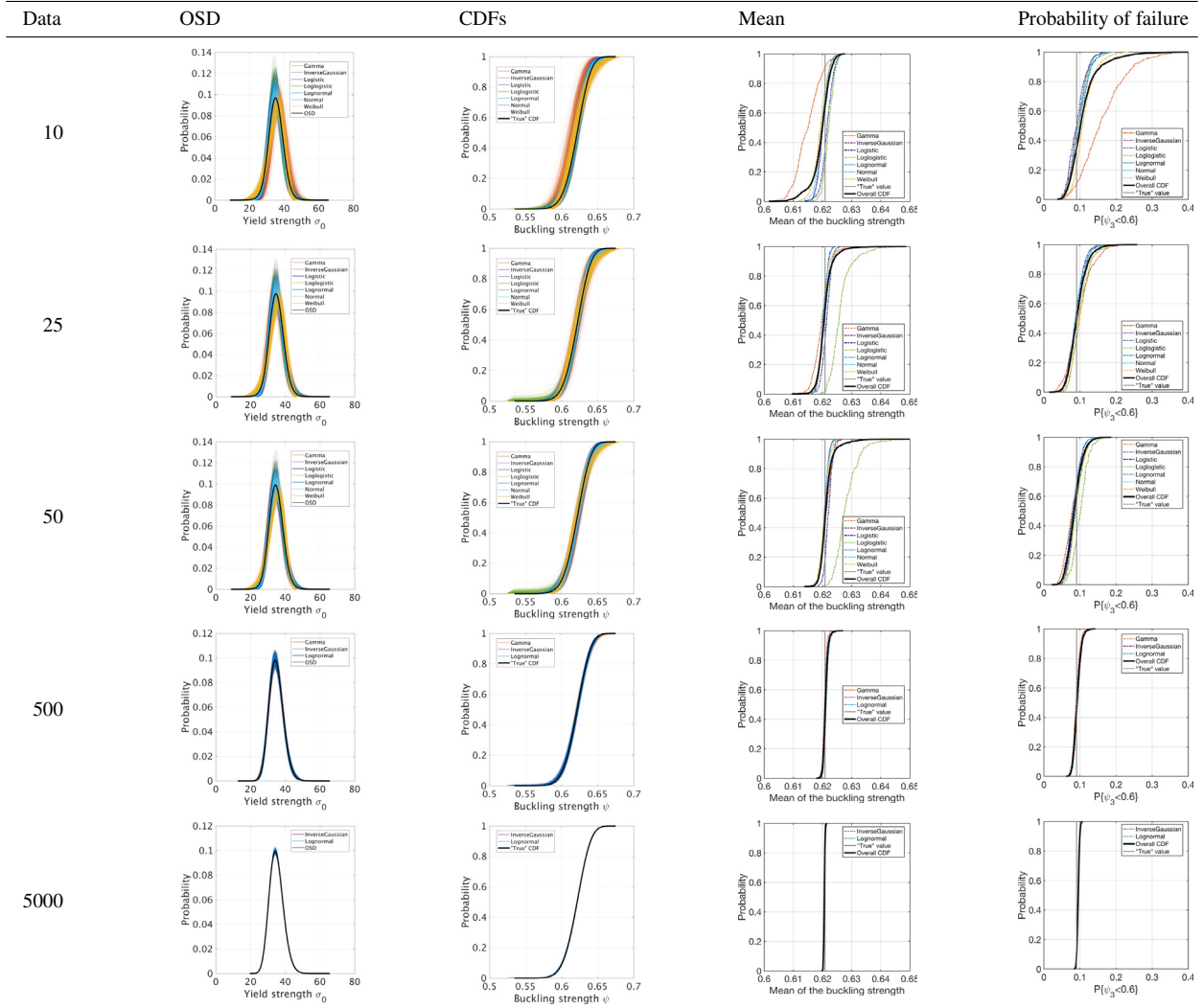
Let us begin by investigating the effect of the prior model probability while retaining the correct ABS-B parameter prior. Fig. 10 shows convergence of the confidence metric (Eq. (34)) and the area accuracy metric (Eq. (35)). These figures show that the strong correct model prior probabilities provide significant improvements in both confidence and accuracy for the mean buckling strength and variance of buckling strength for small datasets. The improvement diminishes as the dataset size increases. For P_f , on the other hand, the prior probabilities have relatively modest effect on convergence.

Next, consider the effect of the parameter priors. Here, we employ equal prior model probabilities and vary the parameter prior. Fig. 11 shows convergence of the confidence and area metrics for the mean buckling strength, variance of buckling strength, and P_f with dataset size. As expected, we see that the ABS-B prior shows consistently good performance in terms of both confidence and accuracy (it is a good prior). In fact, most of the other priors show reasonable performance as well and all converge in confidence at approximately the same rate. The problem lies in the accuracy convergence of the mean buckling strength and P_f using the ASTM-A7 and ABS-A priors. Recall that these models did not accurately quantify input uncertainty. Consequently, the accuracy of response statistics is slow to converge.

This poses a significant problem because Fig. 11a–c suggest a high level of confidence regardless of the prior but d–f suggest that accuracy depends on the prior. The result in these cases is high confidence in inaccurate statistics.

Table 8

Optimal sampling density (OSD), CDFs, mean and probability of failure for ABS-B prior associated with equal model prior probability as a function of dataset size from 10, 25, 50, 500, to 5000.



This is more clearly illustrated in Fig. 12, which shows CDFs for the mean buckling strength and P_f for different priors given 10,000 data with equal prior model probabilities. In the mean value, the CDF for the ASTM-A7 prior is narrow but does not intersect the true value. Quantitatively, its confidence metric is small suggesting 95% probability that the value lies in the range [0.61979, 0.62036] but is inaccurate as the true value is $\mu_\psi = 0.62089$. Similarly, the ASTM-A7 and ABS-A priors yield high confidence in incorrect P_f estimates. Their values of 95% probability lie in the range [0.07249, 0.07974] and [0.09758, 0.10725] respectively but are both inaccurate given that the true value is $P_f = 0.090132$. The result using these priors, even for large datasets, is high confidence in the wrong answer.

6.4. Discussion

The objective of imprecise probabilities in general, and the Bayesian multimodel UQ and propagation method proposed here more specifically, is to provide a near-complete picture of both epistemic and aleatory uncertainty in computational modeling. While the presented methodology is robust under noninformative priors, the work here has shown that it is not immune to biases introduced by improperly informed priors. Even with only slight mis-information in the prior (e.g. materials data that are from similar but not identical materials), the Bayesian approach can produce

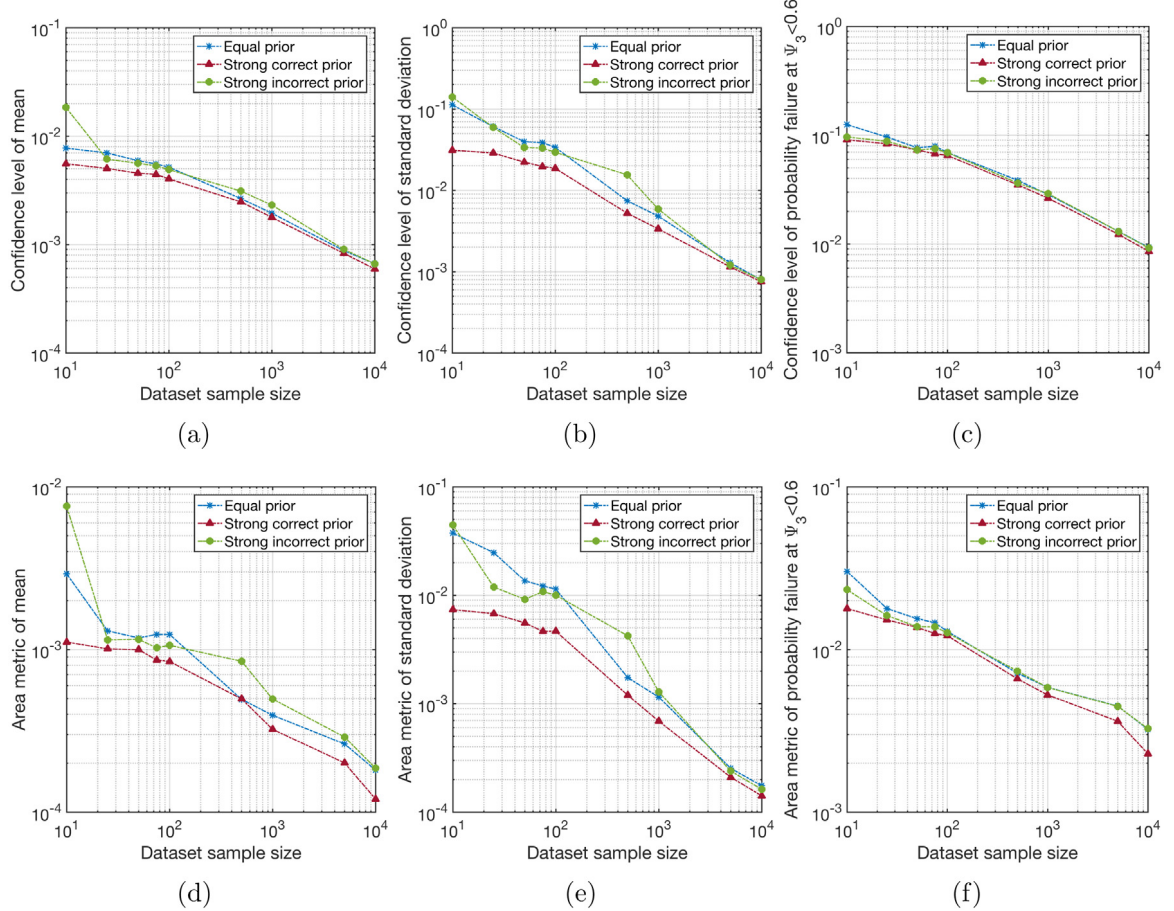


Fig. 10. Compare the effect of prior model probability for ABS-B prior — convergence of confidence level of (a) mean, (b) variance, (c) probability of failure; and area validation metric for (d) mean, (e) variance and (f) probability of failure.

erroneous results that propagate through the computational modeling process yielding incorrect predictions of system performance and probability bounds that do not include the true response. Noninformative priors, while robust in bounding the real uncertainties, may be unnecessarily wide when compared to properly informed priors when datasets are small (for large datasets there is little benefit to informative priors). Consequently, it is the modelers responsibility to judge the relative “safety” of using noninformative priors with the risk and benefits of using informative priors.

7. Conclusion

In this work, the multimodel uncertainty quantification and propagation method previously proposed by the authors [23] is recast in a fully Bayesian framework. This provides additional robustness in terms of quantifying uncertainties associated with probability model form in particular. Within this Bayesian framework, we are primarily interested in understanding the influence of prior probabilities in both probability model-form and probability model parameters on multimodel UQ and the propagation of these uncertainties.

The paper deals primarily with the case where uncertainties are quantified from small datasets, which necessitates a multimodel approach and makes prior probabilities important. Through an example considering the analytical buckling analysis of a simply supported plate, we systematically explore the effect of various prior model-form and model parameter probabilities on multimodel uncertainty quantification and propagation. With regard to model-form uncertainties, it is shown that assumptions about prior probabilities have a significant influence on quantified uncertainties when datasets are small but incorrect prior probabilities can be overcome by large datasets if the

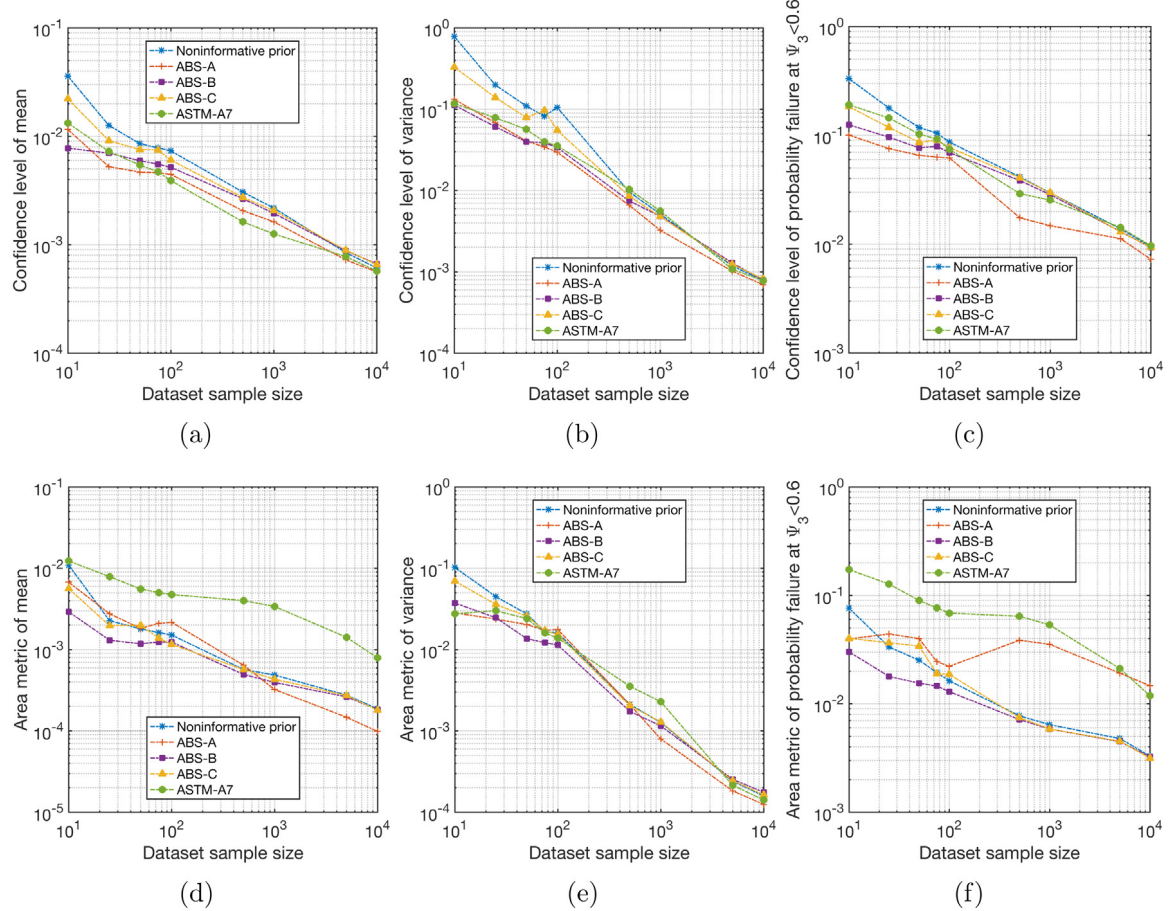


Fig. 11. Equal prior model probability and different parameter priors — convergence of confidence level of (a) mean, (b) variance and (c) probability of failure; and area validation metric for (d) mean, (e) variance and (f) probability of failure.

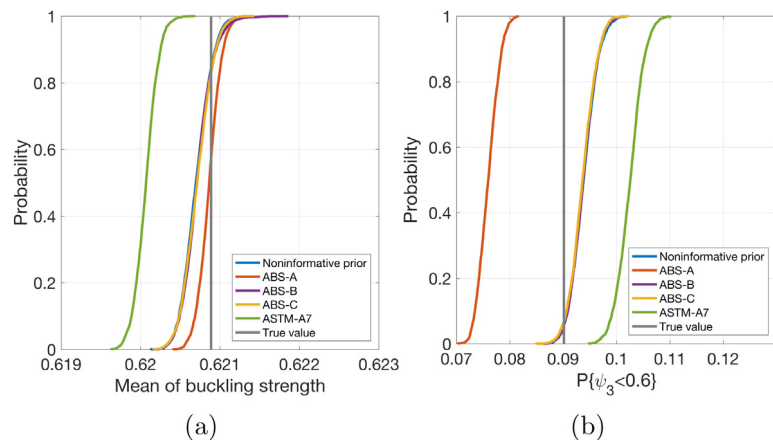


Fig. 12. Empirical CDFs of (a) mean of buckling strength and (b) probability of failure at $\psi_3 < 0.6$ given 10 000 data with equal prior model probability for different parameter priors.

parameter priors are appropriate. With regard to model parameter priors, it is shown that priors derived from historical datasets of varying suitability to the present analysis have a clear influence on uncertainties quantified from small datasets. Moreover, parameter priors derived from historical datasets that are similar to the presently collected data (but nonetheless different) can introduce biases in the multimodel inference that persist even as very large datasets are collected.

The combined effects of model-form and model parameter priors on uncertainty propagation are then investigated. Again, it is shown that uncertainties in response quantities depend strongly on both priors and biases introduced by incorrect priors persist yielding inaccurate probabilistic response quantities even in the large data limit.

Acknowledgment

The work presented herein has been supported by the Office of Naval Research under Award Number N00014-16-1-2582 with Dr. Paul Hess as program officer.

References

- [1] A. Der Kiureghian, O. Ditlevsen, Aleatory or epistemic? Does it matter? *Struct. Saf.* 31 (2) (2009) 105–112.
- [2] P. Walley, Statistical Reasoning with Imprecise Probabilities, Vol. 42, Peter Walley, 1991.
- [3] P. Walley, Towards a unified theory of imprecise probability, *Internat. J. Approx. Reason.* 24 (2–3) (2000) 125–148.
- [4] I. Molchanov, Theory of Random Sets, Vol. 53, Springer-Verlag, London, 2005.
- [5] T. Fetz, M. Oberguggenberger, Propagation of uncertainty through multivariate functions in the framework of sets of probability measures, *Reliab. Eng. Syst. Saf.* 85 (1–3) (2004) 73–87.
- [6] T. Fetz, M. Oberguggenberger, Imprecise random variables, random sets, and monte carlo simulation, *Internat. J. Approx. Reason.* 78 (2016) 252–264.
- [7] R.E. Moore, Methods and Applications of Interval Analysis, Vol. 2, SIAM, 1979.
- [8] K. Weichselberger, The theory of interval-probability as a unifying concept for uncertainty, *Internat. J. Approx. Reason.* 24 (2) (2000) 149–170.
- [9] S. Ferson, V. Kreinovich, L. Ginzburg, D.S. Myers, K. Sentz, Constructing Probability Boxes and Dempster-Shafer Structures, Vol. 835, Sandia National Laboratories, Albuquerque, 2002.
- [10] S. Ferson, J.G. Hajagos, Arithmetic with uncertain numbers: rigorous and (often) best possible answers, *Reliab. Eng. Syst. Saf.* 85 (1) (2004) 135–152.
- [11] R. Schöbi, B. Sudret, Uncertainty propagation of p-boxes using sparse polynomial chaos expansions, *J. Comput. Phys.* 339 (2017) 307–327.
- [12] A.E. Raftery, Bayesian model selection in social research, in: *Sociological Methodology*, 1995, pp. 111–163.
- [13] S. Sankararaman, S. Mahadevan, Distribution type uncertainty due to sparse and imprecise data, *Mech. Syst. Signal Process.* 37 (1) (2013) 182–198.
- [14] P. Walley, T.L. Fine, Towards a frequentist theory of upper and lower probability, *Ann. Statist.* (1982) 741–761.
- [15] M.E. Cattaneo, Empirical interpretation of imprecise probabilities, in: Proceedings of the Tenth International Symposium on Imprecise Probability: Theories and Applications, 2017, pp. 61–72.
- [16] D. Dubois, H. Prade, Random sets and fuzzy interval analysis, *Fuzzy Sets and Systems* 42 (1) (1991) 87–101.
- [17] D. Dubois, H. Prade, Interval-valued fuzzy sets, possibility theory and imprecise probability, in: EUSFLAT Conf., 2005, pp. 314–319.
- [18] D. Dubois, H. Prade, Possibility Theory: An Approach to Computerized Processing of Uncertainty, Springer Science & Business Media, 2012.
- [19] A.P. Dempster, Upper and lower probabilities induced by a multivalued mapping, *Ann. Math. Statist.* (1967) 325–339.
- [20] G. Shafer, A Mathematical Theory of Evidence, Vol. 1, Princeton University Press, Princeton, 1976.
- [21] L.A. Zadeh, Fuzzy sets, *Inf. Control* 8 (3) (1965) 338–353.
- [22] M. Beer, S. Ferson, V. Kreinovich, Imprecise probabilities in engineering analyses, *Mech. Syst. Signal Process.* 37 (1) (2013) 4–29.
- [23] J. Zhang, M.D. Shields, On the quantification and efficient propagation of imprecise probabilities resulting from small datasets, *Mech. Syst. Signal Process.* 98 (2018) 465–483.
- [24] D. Draper, Assessment and propagation of model uncertainty, *J. R. Stat. Soc. Ser. B Stat. Methodol.* (1995) 45–97.
- [25] D. Draper, J.S. Hodges, E.E. Leamer, C.N. Morris, D.B. Rubin, A research agenda for assessment and propagation of model uncertainty, 1987.
- [26] T.K. Dijkstra, On Model Uncertainty and its Statistical Implications: Proceedings of a Workshop, Held in Groningen, The Netherlands, September 25–26, 1986, Vol. 307, Springer Science & Business Media, 1988.
- [27] J.L. Beck, K.-V. Yuen, Model selection using response measurements: Bayesian probabilistic approach, *J. Eng. Mech.* 130 (2) (2004) 192–203.
- [28] J.L. Beck, Bayesian system identification based on probability logic, *Struct. Control Health Monit.* 17 (7) (2010) 825–847.
- [29] S.H. Cheung, J.L. Beck, Calculation of posterior probabilities for bayesian model class assessment and averaging from posterior samples based on dynamic system data, *Comput.-Aided Civ. Infrastruct. Eng.* 25 (5) (2010) 304–321.
- [30] K. Farrell, J.T. Oden, D. Faghihi, A Bayesian framework for adaptive selection, calibration, and validation of coarse-grained models of atomistic systems, *J. Comput. Phys.* 295 (2015) 189–208.
- [31] J.T. Oden, E.A. Lima, R.C. Almeida, Y. Feng, M.N. Rylander, D. Fuentes, D. Faghihi, M.M. Rahman, M. DeWitt, M. Gadde, et al., Toward predictive multiscale modeling of vascular tumor growth, *Arch. Comput. Methods Eng.* 23 (4) (2016) 735–779.

- [32] E. Prudencio, P. Bauman, D. Faghihi, K. Ravi-Chandar, J. Oden, A computational framework for dynamic data-driven material damage control, based on Bayesian inference and model selection, *Internat. J. Numer. Methods Engrg.* 102 (3–4) (2015) 379–403.
- [33] H. Akaike, A new look at the statistical model identification, *IEEE Trans. Automat. Control* 19 (6) (1974) 716–723.
- [34] H. Akaike, Canonical correlation analysis of time series and the use of an information criterion, *Math. Sci. Eng.* 126 (1976) 27–96.
- [35] G. Schwarz, et al., Estimating the dimension of a model, *Ann. Statist.* 6 (2) (1978) 461–464.
- [36] C.M. Hurvich, C.-L. Tsai, Regression and time series model selection in small samples, *Biometrika* 76 (2) (1989) 297–307.
- [37] S. Konishi, G. Kitagawa, *Information Criteria and Statistical Modeling*, Springer Science & Business Media, 2008.
- [38] C. Chatfield, Model uncertainty, data mining and statistical inference, *J. Roy. Statist. Soc. Ser. A* 158 (3) (1995) 419–466.
- [39] J.A. Hoeting, D. Madigan, A.E. Raftery, C.T. Volinsky, Bayesian model averaging: a tutorial, *Statist. Sci.* (1999) 382–401.
- [40] K.P. Burnham, D.R. Anderson, Multimodel inference understanding aic and bic in model selection, *Sociol. Methods Res.* 33 (2) (2004) 261–304.
- [41] H. Akaike, Likelihood of a model and information criteria, *J. Econometrics* 16 (1) (1981) 3–14.
- [42] C.M. Hurvich, C.-L. Tsai, Model selection for extended quasi-likelihood models in small samples, *Biometrics* (1995) 1077–1084.
- [43] S. Chib, I. Jeliazkov, Marginal likelihood from the metropolis–hastings output, *J. Amer. Statist. Assoc.* 96 (453) (2001) 270–281.
- [44] J. Skilling, Nested sampling, in: *AIP Conference Proceedings*, Vol. 735, AIP, 2004, pp. 395–405.
- [45] C.S. Bos, A comparison of marginal likelihood computation methods, in: *Compstat*, Springer, 2002, pp. 111–116.
- [46] N. Friel, J. Wyse, Estimating the evidence—a review, *Stat. Neerl.* 66 (3) (2012) 288–308.
- [47] Z. Zhao, T.A. Severini, Integrated likelihood computation methods, *Comput. Statist.* (2016) 1–33.
- [48] W.K. Hastings, Monte carlo sampling methods using markov chains and their applications, *Biometrika* 57 (1) (1970) 97–109.
- [49] S. Geman, D. Geman, Stochastic relaxation, gibbs distributions, and the bayesian restoration of images, *IEEE Trans. Pattern Anal. Mach. Intell.* (6) (1984) 721–741.
- [50] J. Goodman, J. Weare, Ensemble samplers with affine invariance, *Commun. Appl. Math. Comput. Sci.* 5 (1) (2010) 65–80.
- [51] D. Foreman-Mackey, D.W. Hogg, D. Lang, J. Goodman, Emcee: The mcmc hammer, *Publ. Astron. Soc. Pac.* 125 (925) (2013) 306.
- [52] J. Zhang, M. Shields, Probability measure changes in monte carlo simulation, In Review, Probabilistic Engineering Mechanics, 2017.
- [53] H. Chipman, E.I. George, R.E. McCulloch, M. Clyde, D.P. Foster, R.A. Stine, *The Practical Implementation of Bayesian Model Selection*, in: *Lecture Notes-Monograph Series*, 2001, pp. 65–134.
- [54] J.O. Berger, J.M. Bernardo, Estimating a product of means: Bayesian analysis with reference priors, *J. Amer. Statist. Assoc.* 84 (405) (1989) 200–207.
- [55] A. Gelman, et al., Prior distributions for variance parameters in hierarchical models (comment on article by browne and draper), *Bayesian Anal.* 1 (3) (2006) 515–534.
- [56] L. Tenorio, *An Introduction to Data Analysis and Uncertainty Quantification for Inverse Problems*, Vol. 3, SIAM, 2017.
- [57] H. Jeffreys, An invariant form for the prior probability in estimation problems, in: *Proceedings of the Royal Society of London A: Mathematical, Physical and Engineering Sciences*, Vol. 186, The Royal Society, 1946, pp. 453–461.
- [58] D.W. Scott, *Multivariate Density Estimation: Theory, Practice, and Visualization*, John Wiley & Sons, 2015.
- [59] B.W. Silverman, *Density Estimation for Statistics and Data Analysis*, Vol. 26, CRC press, 1986.
- [60] N. Class, Investigation report on structural safety of large container ships, 2014.
- [61] D. Faulkner, A review of effective plating to be used in the analysis of stiffened plating in bending and compression, *Tech. rep.* 1973.
- [62] C.A. Carlsen, Simplified collapse analysis of stiffened plates, *Norw. Marit. Res.* 5 (4) (1977).
- [63] P.E. Hess, D. Bruchman, I.A. Assakkaf, B.M. Ayyub, Uncertainties in material and geometric strength and load variables, *Nav. Eng. J.* 114 (2) (2002) 139–166.
- [64] C.G. Soares, Uncertainty modelling in plate buckling, *Struct. Saf.* 5 (1) (1988) 17–34.
- [65] A. Mansour, H. Jan, C. Zigelman, Y. Chen, S. Harding, Implementation of reliability methods to marine structures, *Trans.-Soc. Nav. Archit. Mar. Eng.* 92 (1984) 353–382.
- [66] K. Atua, I. Assakkaf, B.M. Ayyub, Statistical characteristics of strength and load random variables of ship structures, in: *Probabilistic Mechanics and Structural Reliability, Proceeding of the Seventh Specialty Conference*, Worcester Polytechnic Institute, Worcester, Massachusetts, 1996.
- [67] J. Kufman, M. Prager, Marine structural steel toughness data bank. volume 1–4, Tech. rep., DTIC Document, 1990.
- [68] J. Gabriel, E. Imbembo, Investigation of the notch-toughness properties of abs ship platesteels, Tech. rep., Ship Structure Committee Washington DC, 1962.
- [69] I. Boulger, W. Hansen, The effectof metallurgical variables ship-plate steelson the transition temperatures in the drop-weight 1 and charpy v-notch tests, 1962.
- [70] S. Person, W.L. Oberkampf, L. Ginzburg, Model validation and predictive capability for the thermal challenge problem, *Comput. Methods Appl. Mech. Engrg.* 197 (29) (2008) 2408–2430.
- [71] C.J. Roy, W.L. Oberkampf, A comprehensive framework for verification, validation, and uncertainty quantification in scientific computing, *Comput. Methods Appl. Mech. Engrg.* 200 (25) (2011) 2131–2144.